Title
Intestinal inflammation breaks established immune tolerance to a skin commensal

Author
Merana, Geil Ramvielle

Publication Date
2021

Peer reviewed|Thesis/dissertation

Intestinal inflammation breaks established immune tolerance to a skin commensal

by
Geil Ramvielle Merana

DISSERTATION
Submitted in partial satisfaction of the requirements for degree of
DOCTOR OF PHILOSOPHY

in

Biomedical Sciences

in the

GRADUATE DIVISION
of the
UNIVERSITY OF CALIFORNIA, SAN FRANCISCO

Approved:

DocuSigned by:
Clifford Lowell
1EA1A95C4F734C7...

Clifford Lowell
Chair

DocuSigned by:
Tiffany C. Scharschmidt
DocuSigned by:
Averil Ma
DocuSigned by:
Susan Lynch
1A38FCA893D34C5...

Tiffany C Scharschmidt

Averil Ma

Susan Lynch

Committee Members

Dedication

This dissertation is dedicated to

Gil and Genaline Merana,

for raising me in a loving home;

Gil Jr. and Gilliane Merana,

for inspiring me through their own special brilliance;

and

Atahualpa Contreras,

for wholeheartedly supporting this journey through all the twists and turns.

Acknowledgements

I am immensely grateful for each and every person who has inspired and contributed to this journey. Without them, this would not have been possible.

Thank you to my thesis committee members, Drs. Susan Lynch, Averil Ma, and Clifford Lowell, for your scientific advice, utmost support, and infectious passion for research. To my thesis advisor, Dr. Tiffany Scharschmidt, thank you for supporting me through a difficult research project and for seeing in me the potential that I struggled to acknowledge these past few years. You have truly set the standard for the scientist I aim to be: resourceful, tenacious, composed, yet infinitely kind. To all current and previous members of the Scharschmidt Lab, thank you for being a great team to work with and for your ultimate show of love: helping me chop up mouse skin while humoring my interest in intestinal immunity. To all the amazing scientists and staff within HSW12, and elsewhere at UCSF, thank you for all your unparalleled support and friendship.

I would also like to thank former mentors who helped me pursue graduate school, as without them I wouldn't be here in the first place. Dr. Laurent Dejean, thank you for reinvigorating my interest in research and nourishing my scientific ideas even at an early stage. Lilia De La Cerda and Lisa Noble, thank you for helping me navigate the path towards undergraduate research and graduate school, as well as for making the LSAMP office my "home away from home". Dr. Joseph Gandler, thank you for imparting in me the joy of teaching and doing science. Dr. Jeoung-Sook Shin, thank you for taking a huge risk and letting me into your lab at UCSF despite my lack of immunology

experience. To all my current and previous mentors, thank you for believing in my capacity to grow as a scientist, even when others (and even I) had some reservations.

Finally, I would like to thank my loved ones for bringing me much-needed sunshine after weathering the storms. Thank you to my family, and especially my grandparents, who overcame so many odds and still serve as my inspiration to this day. Thank you to my aunts and uncles who took care of me whenever my parents were working. To my parents, Genaline and Gil, thank you for raising me in a home where I always felt loved and accepted. Thank you for your unparalleled belief in my abilities and for supporting my career and life aspirations even if they exist outside cultural norms. To my younger siblings, Gilliane and Gil Jr., thank you for your unconditional love and understanding. To my childhood friends, Kenny and Sam, who have stuck around despite my constant re-scheduling and petty complaining, thank you for sharing endless laughter and for going on adventures with me.

Last but not least, I thank my husband, Atahualpa, for his unwavering love and support. Thank you for being a great cook, a shoulder to cry on, and an irreplaceable exploration buddy. You were always there for me when I needed you the most, even when you were also struggling. I will never forget your endless persistence in soul-sucking jobs just so I could continue to pursue graduate school…because of this, I will never take this career for granted. Even though I am glad to be done with the PhD, I am incredibly excited to see you forge your own path as a scientist.

Contributions

The work presented in this dissertation was performed under the direct supervision and guidance of my thesis advisor, Dr. Tiffany C. Scharschmidt, M.D. Additional guidance and insight were provided by thesis committee members Dr. Clifford Lowell, M.D., Ph.D., Dr. Averil Ma, M.D., and Dr. Susan V. Lynch, Ph.D.

Chapters 2 and 3 of this work are largely adopted from a manuscript in revision: Merana GM, Dhariwala MO, Dwyer LR, Weckel A, Gonzalez JR, Palacios-Calderon Y, Kattah MG, Tasoff P, Ha CWY, Ma A, Lynch SV, Scharschmidt TC. Intestinal inflammation breaks established immune tolerance to a skin commensal (2021). *In revision*. I performed all experiments and data analysis, prepared figures, and wrote the manuscript, with help from Dr. T.C. Scharschmidt. Dr. M.O. Dhariwala, L.R. Dwyer, Dr. A. Weckel, J.R. Gonzalez, and Y. Palacios-Calderon assisted with experiments and manuscript editing. P. Tasoff, Dr. C.W.Y. Ha, and Dr. S.V. Lynch provided their expertise with profiling of microbial communities. Dr. M.G. Kattah and Dr. A. Ma were instrumental in the execution of the A20 Abin colitis model.

Intestinal inflammation breaks established immune tolerance to a skin commensal

Geil Ramvielle Merana

ABSTRACT

The gut and skin are major barrier tissues that house microbial communities capable of influencing host immunity. Under homeostatic conditions, resident microbes at each of these two sites are thought to have a dominant impact on local immune cell function. However, the prevalence of neutrophilic skin disorders among patients with Inflammatory Bowel Disease suggests that this compartmentalized control may not hold under disease conditions. We hypothesized that an altered immune response to gut-resident microbes during colitis may facilitate excessive inflammation directed at skin commensals. Using an established model, wherein neonatal colonization by *Staphylococcus epidermidis* facilitates development of adaptive immune tolerance and enrichment in *S. epidermidis*-specific $CD4^+$ regulatory T cells (Tregs), we asked whether this tolerance to skin bacteria can be perturbed in the context of gut inflammation. Induction during adulthood of either chemically or genetically-mediated colitis, but not systemic inflammation alone, led to reduced percentages of *S. epi*-specific Tregs in skin and skin-draining lymph nodes (LN) and an increase in skin neutrophils. Intestinal presence of *S. epidermidis* and reduced percentages of *S. epidermidis*-specific Tregs at this site during colitis suggested initiation of this altered response in the gut. Consistent with this, adoptive transfer and photoconversion experiments revealed a colitis-induced increase in $CD4^+$ T cell trafficking from gut-draining LN to skin-draining LN. Recovery in

the percentage of *S. epidermidis*-specific Tregs in colitic *Cd4*^{cre}*Il1r1*$^{fl/fl}$ mice further indicated a role for circulating IL-1 cytokines in shifting the CD4^{+} skin commensal response during colitis. Collectively, these results identify a context in which there is breakdown in homeostatic separation of skin and gut host-microbe interactions and provide mechanistic insight into observed connections between inflammatory skin and intestinal diseases.

“Bringing my face close to the glass, I looked out at the wide expanse of ocean. The horizon seemed to be pushing up against the sky. I followed the line where the sky met the water from end to end. No human being could draw a line so beautiful, whatever ruler they might use.”

—Haruki Murakami, *Killing Commendatore*

Table of Contents

List of Figures

CHAPTER 1: INTRODUCTION

1.1 The intestines and skin are home to distinct cellular compartments

The intestines and skin are major barrier tissues that play a critical role in coordinating responses to environmental stimuli through a variety of cell types residing in specialized structures. The intestinal tract consists of several mucosal organs from the oral cavity, down to the small and large intestines and their respective draining lymph nodes (the “gut”) (Esterházy et al., 2019; Houston et al., 2016). A one cell layer-thick barrier comprised of columnar intestinal epithelial cells (IECs) separates the mucus-covered lumen—where primary exposure to microbial and food antigens occurs—from the lamina propria, where the majority of intestinal immune cells reside and function (Agace and McCoy, 2017; Brown and Esterházy, 2021). Subsets of epithelial cells reside in the intestinal barrier, encompassing functions ranging from secretory (goblet cells) to absorptive (enterocytes), or even immune-like (Tuft cells). A pool of stem cells at the base of the intestinal crypts supports constant renewal of these populations (Coates et al., 2019).

Meanwhile, the physical barrier of the skin consists of a stratified squamous epithelium made up of keratinocytes that differentiate into specialized populations. In the outermost layer of the skin, the stratum corneum, lipids form a matrix between corneocytes or keratinized cell envelopes. In deeper epidermal layers, the stratum granulosum and stratum spinosum, keratin filaments provide structural support. Stem cells that replenish these populations reside in the basal layer of the epidermis and within hair follicles (Coates et al., 2019).

The intestinal tract and skin also harbor both unique and shared immune cell types in addition to non-immune populations. Intra-epithelial lymphocytes reside in the intestinal epithelial border in close contact with luminal antigens, where their localization and function is influenced by commensal microbes (Hoytema van Konijnenburg et al., 2017). Likewise, gut-resident CX3CR1-expressing mononuclear phagocytes extend their dendrites through the epithelium to “sample” luminal microbial antigens and relay information to intestinal T cells (Niess et al., 2005). In the skin, Langerhans cells strategically reside in the epidermal layer to serve as the first line of defense against pathogens (Merad et al., 2008).

Despite notable differences in specialized subsets of immune cells, the gut and skin are both home to T cells, which are important in maintaining homeostatic interactions with commensal microbes inhabiting these barrier tissues. Belonging to the adaptive arm of the immune system, T cells express unique T cell receptors (TCRs) specific to molecules called antigens, allowing them to undergo activation and expansion upon exposure, and in turn elicit a robust memory response upon re-exposure to the same stimuli. The two main subsets of $CD4^+$ T cells, regulatory and effector, will be the main focus of this dissertation.

1.1.1 Regulatory T cells

Making up only 5-7% of $CD4^+$ T cells in the body as a whole (Raffin et al., 2020), regulatory T cells (Tregs) express the lineage-defining transcription factor Foxp3, a master regulator in their development (Fontenot et al., 2003; Hori et al., 2003; Khattri et

al., 2003). Considered the “overseers” of the immune system, Tregs are especially poised to suppress other cell types, such as effector T cells, in order to maintain homeostasis. Tregs dampen inflammation through mechanisms that are either contact-dependent (checkpoint inhibition molecules such as CTLA-4) or contact-independent (release of cytokines such as IL-10) (Raffin et al., 2020).

The importance of functional Tregs in both mice and humans is underscored by severe autoimmune diseases, such as Immunodysregulation polyendocrinopathy enteropathy X-linked (or IPEX) syndrome, driven by mutations in the Foxp3 gene (Bacchetta et al., 2006). This is further strengthened by early seminal work beginning with the ability of Tregs to prevent inflammation in murine models (Powrie et al., 1993) as well as recent clinical data on their therapeutic potential in various diseases (Raffin et al., 2020). Additionally, Tregs are important in the process of tissue repair, as the absence of these cells can severely blunt timely wound healing (Mathur et al., 2019) or lead to fibrosis (Kalekar et al., 2019). On the other hand, Tregs can be detrimental depending on disease state, as they may suppress the ability of effector T cells that would otherwise attack tumors (Tanaka and Sakaguchi, 2019).

Once thought to be homogeneous and derived only from the thymus (natural Tregs), Tregs have been shown to have heterogeneity within and between tissues (Wing et al., 2019) and have the capacity to be induced outside the thymus (peripheral or induced Tregs) as a response to environmental stimuli. In fact, commensal microbes serve as a significant driving force for peripheral Treg induction in some tissues (Muñoz-

Rojas and Mathis, 2021). These characteristics highlight the importance of studying Tregs in different contexts, especially their role in maintaining appropriate and lasting relationships with commensal microbes.

1.1.2 Th17 cells

Along with Th1 and Th2 cells, T helper type 17 (Th17) cells are specialists within the effector $CD4^+$ T cell (Teff) subset and are important in polarizing immune responses to specific stimuli (Harrington et al., 2005; Park et al., 2005). While Th1 and Th2 cells are known to target pathogenic viruses and helminths respectively, Th17 cells are vital to the body's defense against extracellular bacteria and fungi. As such, defects in Th17 immunity can lead to recurring infections from pathogens such as *Candida albicans* (Stockinger and Omenetti, 2017). Th17 cells are characterized by expression of the transcription factor RORγt and production of the signature cytokine IL-17A (Ivanov et al., 2006). Signals from Th17 cells recruit other immune cells such as neutrophils to sites of inflammation to help combat pathogenic microbes.

However, Th17 cells and the resulting downstream immune responses induced by them can also be pathogenic in other settings, as they have long been implicated in autoimmunity (Langrish et al., 2005). The signature Th17 cytokine IL-17A has been a major therapeutic target in diseases such as Inflammatory Bowel Disease (IBD), psoriasis, rheumatoid arthritis, and multiple sclerosis (Gaffen et al., 2013). The dichotomous nature of Th17 cells in health and disease warrants further investigation, especially in their role in balancing appropriate relationships with commensal microbes.

1.2 Commensal microbes influence the host immune system

Tens of trillions of bacteria, fungi, and viruses reside within an organism's body in tissues such as the intestines and skin. Under homeostatic settings, microbes considered to be "commensal" fail to stimulate inflammatory responses and instead are welcomed with features of immune tolerance. Traditionally, this failure to elicit inflammation was thought to stem from "ignorance", or the host's impaired ability to detect commensal microbes (Macpherson and Harris, 2004). However, more recent studies have challenged this idea, instead supporting the paradigm in which calculated exposures drive specific signaling pathways and mold favorable relationships between the host and its resident microbiota (Tuganbaev et al., 2021). Remarkably, microbes can co-opt mechanisms of host immunity in order to facilitate commensalism in the gut (Donaldson et al., 2018) and help protect against sepsis (Wilmore et al., 2018). In addition, there is increasing evidence for the role of the microbiome in directly regulating host immune responses to insults such as skin injury (Di Domizio et al., 2020) as well as influencing therapeutic outcomes (Gopalakrishnan et al., 2018; Nayak et al., 2021).

1.2.1 Diverse microbial communities reside in the gut and skin

The orchestration of host-commensal microbe interactions depends on tissue-specific factors, such as microbial composition. Likewise, the unique composition of commensal microbial communities between the gut and skin is dictated by differences in organ architecture and nutrient availability. The moist, carbon- and nitrogen-rich intestines have a neutral pH and provide a highly anaerobic environment on the surface near the lumen, while the deeper areas of the intestinal crypts are more oxygenated. In

comparison, the surface of the skin is an acidic, high-salt, and dry aerobic environment while its invaginations are lipid-rich and comparatively anaerobic (Chen et al., 2018).

Microbes are not uniformly distributed in both barrier tissues. Microbial burden steadily increases along the intestinal tract, as the speed of transit through the small intestine favors rapidly dividing microbes such as Proteobacteria while a slower flow in the colon allows for microbial metabolism of plant matter by *Bacteroides* and *Clostridia* species, resulting in greater species richness. Even within the colon itself, microbes like *Akkermansia muciniphila* prefer to reside within mucin-rich layers while segmented filamentous bacteria (SFB) directly adhere to epithelial cells (Tropini et al., 2018).

Similarly, specialized niches within the skin harbor distinct microbial communities (Grice et al., 2009; Findley et al., 2013). Lipophilic microbes including *Propionibacterium* species dominate sebaceous sites whereas *Staphylococcus* and *Corynebacterium* species thrive in humid environments such the moist areas of the elbows and feet (Byrd et al., 2018). Interestingly, despite being at the frontline of relentless environmental perturbations, microbial communities are largely stable in both the gut (Faith et al., 2013) and the skin (Oh et al., 2016), where the majority of strains in an individual's microbiota can persist for years, perhaps owing in part to a combination of homeostatic interactions between community members and the maintenance of immune tolerance mechanisms by commensal-induced T cells.

1.2.2 $CD4^+$ T cell responses to commensal microbes

Mice raised in germ-free conditions are known to have severely impaired immune responses and underdeveloped secondary lymphoid organs, highlighting the role of the microbiome in shaping immune development. More importantly, germ-free mice have an overall reduction in Treg and Th17 numbers (Round and Mazmanian, 2010), while the gut and skin are enriched for commensal-specific Treg and Th17 cells in mice raised in specific pathogen-free (SPF) conditions (Scharschmidt et al., 2015).

1.2.3 Commensal-induced Tregs

Tregs are more abundant in the colon LP and skin (around 40% of $CD4^+$ T cells) compared to lymph nodes (around 10-20%) (Malhotra et al., 2018). Although there is newly-found evidence of thymically-generated gut commensal-specific $CD4^+$ T cells (Zegarra-Ruiz et al., 2021), bacterially-derived molecules such as short chain fatty acids (SCFAs) (Smith et al. 2013) and secondary bile acids (Campbell et al. 2020) have been known to induce extrathymic generation of intestinal Tregs. Though there is burgeoning evidence that skin microbes produce similar Treg-inducing molecules such as SCFAs (Schwarz et al., 2017), less is known about the plethora of microbially-derived molecules that could potentially drive Treg accumulation in the skin. Efforts to characterize these important microbial mediators are ongoing in groups such as ours.

1.2.4 Commensal-induced Th17 cells

Unlike tissues such as the oral mucosa, a large proportion of gut and skin-resident Th17 cells arise from exposure to commensal microbes (Dutzan et al., 2017).

In the gut, Th17 induction by microbes seems to be dependent on the method of colonization, as epithelial cell-adherent SFB, *Citrobacter rodentium*, and *Escherichia coli* all induce a Th17 signature while adhesion-defective mutants fail to do so (Atarashi et al., 2015). In skin, colonization by commensals like *Candida albicans* and *Malassezia furfur* is not associated with fulminant tissue inflammation compared to intradermal injection with the same microbes, but these fungi still elicit the accumulation of Th17 cells in homeostatic settings (Hurabielle et al., 2020). Likewise, Th17 cells are induced upon skin colonization with *Staphylococcus* species (Naik et al., 2015). Upon skin injury, *Staphylococcus*-induced Th17 cells contribute to tissue repair (Harrison et al., 2019), highlighting the role of commensal microbes in building protective immune function.

1.3 Immune tolerance to commensal microbes is established in early life

Extensive advances have been made in understanding the mechanisms by which the microbiome elicits immune responses in adulthood. However, there is growing interest in the importance of childhood exposures to microbes in proper immune development, especially as critical immune mechanisms and establishment of microbial communities within host tissues occur in tandem during this early-life window. Tregs are known to accumulate in skin in parallel with hair follicle development in mice (Scharschmidt et al., 2017) and humans (Dhariwala et al., 2020). There exists a short time interval in which induction of antigen-specific tolerance to commensal microbes occurs in the skin (Scharschmidt et al., 2015) and in the gut (Knoop et al., 2018).

Similarly, the assembly of complex microbial communities begins in early life. Upon birth, the host is inundated with commensal microbes that seed barrier tissues, although recent studies have implicated *in utero* exposure as another potential source of microbial education even earlier on (Rackaitye et al., 2020; Mishra et al., 2021). Thus, a “window” of opportunity exists within this early-life timeframe in which host immune cells encounter and are influenced by pioneering microbial colonizers.

The successful orchestration of host-commensal interactions are important as disruption of these essential, immune tolerance-promoting mechanisms in early life can increase susceptibility to certain diseases in adulthood. For example, antibiotic treatment, which de-stabilizes resident microbial communities, has long been linked to the development of asthma and allergy in humans (Russell et al., 2012) and interrupts the “weaning reaction” in mice, leading to pathological imprinting and increased susceptibility to other diseases such as colitis in later life (Al Nabhani et al., 2019).

1.4 Aims of this study

Current literature has started to explore the role of early-life disruption of host-commensal interactions in disease development. However, less is known about the mechanisms by which factors that emerge in adulthood can undermine established tolerance to commensal microbes and contribute to unexpected pathogenic responses. In addition, current literature on the connections between gut and skin are largely limited to correlative studies regarding the role of intestinal microbial dysbiosis on the development of various skin diseases. As re-programming of immunity is an ongoing

process, the aim of this study is to investigate the cellular and molecular mechanisms by which intestinal-driven inflammation in adulthood can disrupt an intimate host-commensal relationship established in the skin in early life.

CHAPTER 2: Intestinal inflammation alters the cutaneous immune response to a skin commensal microbe

INTRODUCTION

The intestinal tract and skin are two major barrier sites both housing complex microbial communities and resident immune cell populations. In these tissues, adaptive immune tolerance to commensal bacteria is initiated by early life microbial exposures that support expansion of commensal-specific regulatory T cell (Treg) populations (Knoop et al., 2017; Scharschmidt et al., 2015; Scharschmidt et al., 2017). Establishment of this tolerance is critical for later-life immune homeostasis at barrier sites, as is demonstrated by the inflammatory consequences of disrupting early-life host-microbe interactions (Al Nabhani et al., 2019; Russell et al., 2012). Even if appropriately established at birth, there remains the possibility that subsequent loss of adaptive immune tolerance toward microbial antigens could result in increased inflammation and disease at these barrier sites. However, the circumstances and mechanisms that predispose to this loss of commensal-specific tolerance, especially as relates to skin bacteria, remain poorly defined.

Mutualistic relationships between resident immune cells and neighboring microbes in tissues rely on a delicate balance between effector $CD4^+$ T cells (Teff), which produce cytokines to support antimicrobial defense, and $Foxp3^+$ $CD4^+$ regulatory T cells (Tregs) that help restrain excessive inflammatory responses. For a given antigen, the ratio between these two populations, more so than the absolute number of Tregs, appears to be a critical determinant of whether tolerance can prevail and inflammation is kept at bay (Su et al. 2016, Rosenblum et al. 2016). $CD4^+$ T cells responsive to tissue-resident bacteria span a phenotypic continuum (Kiner et al. 2021), influenced by factors including identity of the microbe, timing of colonization, and

concurrent local inflammatory cues (Hand et al. 2012, Leech et al 2019). In the intestinal tract and skin, commensal-specific $CD4^+$ cells tend to be especially enriched for type 17 helper T (Th17) cells and Tregs (Atarashi et al. 2011, Harrison et al. 2019, Ivanov et al. 2009, Round et al. 2010, Scharschmidt et al. 2015).

Under homeostatic conditions, tissue-resident microbes are thought to have a dominant impact on local immune cell function (Belkaid and Harrison, 2017; Durack and Lynch, 2019). According to prevailing dogma, “compartmentalization” exists in healthy hosts between organs such as the intestinal tract and skin, which harbor dense and distinct microbial populations. In a seminal study of these two tissues, neither oral gavage with segmented filamentous bacteria nor antibiotic-mediated depletion of intestinal microbes altered the skin $CD4^+$ T cell compartment in mice. In contrast, skin colonization by the commensal *Staphylococcus epidermidis* (*S. epidermidis*) augmented cutaneous $CD4^+$ T cell numbers and cytokine production (Naik et al. 2012).

However, there is increasing evidence that disease can weaken “compartmentalization” of the intestinal immune response to luminal microbes (Akdis 2021, Ayres 2016). In mice, acute intestinal infection supports systemic dissemination of commensal-specific effector $CD4^+$ T cells (Hand et al. 2012). In humans, alterations in the intestinal microbiome are linked to extra-intestinal diseases including asthma, rheumatoid arthritis, and multiple sclerosis (Durack and Lynch, 2019). Notably, Inflammatory Bowel Disease (IBD), a condition in which genetic and environmental factors fuel microbiome disruption and intestinal inflammation, predisposes patients to

neutrophilic skin dermatoses by poorly understood mechanisms. Although shared genetic features may separately confer risk for simultaneous skin and gut disease (Marzano et al. 2014), there is sufficient evidence for skin inflammation in the setting of gut microbiome perturbation (Myers et al. 2019, Song et al. 2016) to explore a possible role for a disrupted, cross-reactive immune response to microbes at both barriers. First, however, additional mechanistic insight into the relationship between the intestinal tract and skin in the context of host-microbe interactions is needed.

Here, we sought to address whether intestinal inflammation impacts the adaptive immune response to commensal bacteria in the skin. More specifically, by combining our system to track *S. epidermidis*-specific $CD4^+$ Tregs and Teffs following neonatal colonization (Scharschmidt et al., 2015) with two colitis models (Kattah et al., 2018; Wirtz et al. 2017), we set out to test the hypothesis that intestinal inflammation can undermine previously established adaptive immune tolerance to skin commensals. We demonstrate that in adult mice, colitis (but not systemic inflammation) decreases the *S. epidermidis*-specific Treg response in skin and skin-draining lymph nodes and predisposes to neutrophilic skin infiltration. This phenomenon is linked to a concurrent intestinal $CD4^+$ response to *S. epidermidis*, which is augmented and skewed towards Teffs during colitis. We find that colitis predisposes towards gut-to skin trafficking of $CD4^+$ T cells and that inhibition of lymphocyte circulation rescues the skin *S. epidermidis*-specific Treg response. Finally, we identify that excess IL-1R1 signaling in T cells facilitates the reduction in *S. epidermidis*-specific Tregs during colitis. Our results

reveal cell type and pathway-specific mechanisms by which intestinal inflammation impacts established host-microbe relationships in the skin.

RESULTS

2.2.1 Intestinal inflammation disrupts established immune tolerance to *S. epidermidis*

To probe the relationship between intestinal and skin inflammation, we first sought to address whether acute intestinal inflammation spontaneously expands or activates immune cells present in skin and skin-draining lymph nodes (skin-draining LN). To test this, we subjected adult (5-6 week old) wild-type (WT) C57BL/6, specific pathogen-free (SPF) mice to a model of dextran sodium sulfate (DSS)-mediated acute intestinal inflammation (Wirtz et al. 2017). 3.5% DSS was provided to mice in their drinking water for 5 days, which resulted in decreased colon length (**Fig. 2.1A**). At day 10, skin and skin-draining LN were analyzed by flow cytometry to quantify $CD4^+$ T cell populations (**Fig. 2.1B**) as well as myeloid cells (**Fig. 2.2A**). In both organs, no significant differences in DSS-treated mice vs. water-treated controls were seen for the majority of the populations surveyed, including IL-17A or IFNγ-producing $CD4^+$ T cells (**Fig. 2.1C-F**), though there was a minimal difference in the CCR2+ monocytes at the height of disease at day 7 (**Fig. 2.2B**). This suggests that intestinal inflammation alone is largely insufficient to undermine immune compartmentalization of intestinal and skin tissues, especially the $CD4^+$ T cells, in the context of acute murine colitis.

Relying upon the concept of pathergy, in which minor skin trauma leads to exacerbation of existing or development of new skin inflammation (Kutlubay et al., 2017), we tested the effect of an additional skin-directed signal in this same model. The back skin of adult mice was tape-stripped to minimally abrade the epidermis (Scharschmidt 2015) on days 0, 3 and 6 concurrent with DSS or water administration

before harvest on day 10. Tape-stripping revealed a heightened neutrophil response in skin of DSS-treated mice (**Fig. 2.2C-D**) as well as changes in the rest of the myeloid compartment during the treatment period (**Fig. 2.3**), suggesting the possibility that increased exposure to skin commensals may be necessary to uncover a skin response during concurrent intestinal challenge.

We previously showed that neonatal skin colonization with a model antigen (2W)-expressing strain *S. epidermidis (S. epi)*-2W results in establishment of antigen-specific tolerance. This tolerance is denoted by a high percentage of $2W^+$ regulatory T cells (Tregs) in the skin and skin-draining LN upon *S. epi*-2W re-exposure and skin tape-stripping in adult life, which is accompanied by reduced histologic skin inflammation and skin neutrophil infiltration as compared to mice not colonized by *S. epi*-2W during infancy (Scharschmidt 2015). We took advantage of this existing model to test the hypothesis that altered immune responses during colitis may facilitate excessive inflammation directed at skin commensal microbes—resulting in a “breakdown” of previously established tolerance.

To investigate whether acute intestinal inflammation alters the skin immune response to *S. epi*-2W, we colonized WT SPF mice with the bacteria on postnatal days 7, 10, and 13 to establish a Treg-enriched *S. epi*-specific $CD4^+$ compartment as previously demonstrated (Scharschmidt 2015). These mice were then aged to adulthood (5-6 weeks of age), when they were re-challenged with *S. epi*-2W plus tape-stripping, with one experimental group receiving DSS in the drinking water and another receiving

water as a control (**Fig. 2.4A**). As expected from prior literature (Wirtz et al., 2017) the DSS-treated group developed fulminant colitis, with appreciable weight loss (**Fig. 2.4B**) and decreased colon length at harvest on day 10 (**Fig. 2.4C**).

Both groups were able to mount a comparable antigen-specific memory response to *S. epi*-2W (**Fig. 2.4E, top**), as reflected by an equivalent percentage and number of $2W^+CD44^+CD4^+$ T cells in skin-draining LN (**Fig. 2.4F**) and skin (**Fig. 2.4G**). However, the quality of the *S. epi*-specific $CD4^+$ response in DSS-treated mice was notably altered (**Fig. 2.4E, bottom**), with a decreased percentage of *S. epi*-2W specific Tregs evident in both skin-draining LN and skin (**Fig. 2.4H**), as compared to control mice. Interestingly, the percentage of polyclonal Tregs in skin-draining LN and skin (**Fig. 2.4I**) were not reduced in comparison, suggesting that underlying intestinal inflammation plus skin injury can specifically influence commensal-specific $CD4^+$ T cell responses in skin. This reversal in the *S. epi*-specific Treg response was accompanied by an increase in skin neutrophils (**Fig. 2.4J**) and in IL-17A-producing but not IFNγ or IL-13-producing $CD4^+$ T cells in skin (**Fig. 2.4K**), further corroborating the breakdown of established tolerance to skin *S. epidermidis.*

To test whether this breakdown of tolerance was generalizable to other models of colitis, we utilized a genetic model wherein inducible intestinal epithelial cell-specific mutations in two IBD-associated genes, A20 and ABIN-1, results in acute intestinal inflammation (Kattah et al. 2018). $A20^{fl/fl}$ $Abin^{fl/+}$ $Villin\text{-}Cre^{ERT2\ Tg+}$ (*Villin-Cre*$^+$) and $A20^{fl/fl}$ $Abin^{fl/+}$ $Villin\text{-}Cre^{ERT2\ Tg-}$ (*Villin-Cre*$^-$) SPF mice were pre-colonized with *S. epi*-2W

and aged to adulthood (5-6 weeks of age), at which point they were injected with tamoxifen intraperitoneally (i.p.) to induce Cre-mediated recombination and concurrently rechallenged with *S. epi*-2W plus tape stripping as previously described (**Fig. 2.5A**). The *Villin-Cre*$^+$ group developed fulminant colitis, with appreciable weight loss (**Fig. 2.5B**) and decreased colon length (**Fig. 2.5C**) at harvest on day 10. Both groups were able to mount a comparable antigen-specific memory response to *S. epi*-2W, as reflected by an equivalent percentage (**Fig. 2.5D**) and number (**Fig. 2.5E**) of 2W$^+$CD44$^+$CD4$^+$ T cells in skin-draining LN. However, similar to DSS-treated mice, the quality of the *S. epi*-specific CD4$^+$ response in *Villin-Cre*$^+$ mice was notably altered, with a decreased percentage of *S. epi*-2W specific Tregs evident in skin-draining LN (**Fig. 2.5F**) as compared to *Villin-Cre*$^-$ mice, while the percentage of polyclonal Tregs in skin-draining LN remained unchanged (**Fig. 2.5G**).

To further corroborate our findings in another system, we utilized the chronic model of DSS-induced colitis, wherein neonatally-colonized WT mice were subjected to three rounds of DSS treatment before rechallenge with *S. epi*-2W plus tape stripping in the last round of treatment (**Fig. 2.5H**). Similar to the acute DSS model, the quality of the *S. epi*-specific CD4$^+$ response in mice which underwent chronic DSS treatment was notably altered (**Fig. 2.5I**). Collectively, these results demonstrate the robustness of the finding that intestinal inflammation concurrent with skin injury alters commensal-specific CD4$^+$ T cell responses in skin.

Finally, we wondered whether the effects of acute colitis on cutaneous immunity could persist long after initiation of inflammation. To test this initially, we colonized WT SPF mice with the bacteria on postnatal days 7, 10, and 13, then induced colitis three weeks later. After another three weeks post-DSS treatment, mice were re-challenged with *S. epi*-2W plus tape-stripping while receiving regular drinking water (**Fig. 2.6A**). Although the antigen-specific response to *S. epi*-2W was unchanged (**Fig. 2.6B**), there remained a noticeable increase in polyclonal $CD4^+$ T cell and neutrophil response in the skin-draining LN even three weeks past induction of acute colitis (**Fig. 2.6C-E**), suggesting that transient gut inflammation could have lasting consequences on host-microbe relationships.

2.2.2 Systemic inflammation alone is not sufficient to alter the antigen-specific response *to S. epidermidis*

To further probe the mechanisms that break established tolerance to *S. epi*-2W, we then asked whether systemic inflammation alone would be sufficient to alter the antigen-specific response. To test this, we subjected pre-colonized, adult (5-6 week old) WT SPF mice to a modified lipopolysaccharide (LPS)-induced sepsis model. In the LPS-induced sepsis model, mice are typically given one 10 mg/kg dose of LPS resulting in death within 3-4 days (Lehner et al., 2001). We chose this model as it recapitulates the type of systemic inflammation seen in DSS-colitis, i.e., an acute increase in systemic pro-inflammatory cytokines and circulating neutrophils and monocytes (Cao et al., 2019; Napier et al., 2021) but without intestinal barrier breach as the causative event. We modified this model to allow for development of systemic inflammation

through a longer time period of 10 days, which better matched the level of inflammation in the DSS model and allowed us to concurrently assess the *S. epi*-specific $CD4^+$ T cell response. After titrating the LPS to match DSS-induced weight loss, we injected one group of mice intraperitoneally with 2 mg/kg LPS and another group with PBS during the *S. epi*-2W re-challenge period (**Fig. 2.7A**). The LPS-injected mice developed fulminant inflammation, with weight loss (**Fig. 2.7B**) and neutrophilic infiltration into the spleen (**Fig. 2.7C**) and skin-draining LN (**Fig. 2.7D**) at the end (day 10) of the re-challenge period. Both LPS and PBS-injected mice were equally able to mount a memory response to *S. epi*-2W, as reflected by an equivalent percentage (**Fig. 2.7E**) and number (**Fig. 2.7F**) of $2W^+CD44^+CD4^+$ T cells in skin-draining LN. Notably, the quality of the *S. epi*-2W response in LPS-treated mice did not change, with both groups showing an equivalent percentage of *S. epi*-specific Tregs in skin-draining LN (**Fig. 2.7G**) and comparable numbers of skin neutrophils (**Fig. 2.7H**). To test whether repeated LPS exposure could skew the commensal-specific response to *S. epi*-2W, we injected mice i.p. with 1 mg/kg LPS or PBS on days 0, 3, and 6 of the re-challenge period and found that both groups still showed equivalent percentages of *S. epi*-specific Tregs in skin-draining LN (**Fig. 2.7I**).

As DSS-induced colitis results in an excess of systemically circulating gut microbial antigen (Eichele and Kharbanda, 2017), we speculated whether additional antigen from *S. epi*-2W could push this system. To test whether repeated LPS exposure and additional circulating 2W antigen could skew the commensal-specific response to *S. epi*-2W, we injected mice i.p. with 1 mg/kg LPS plus heat-killed *S. epi*-2W or PBS on

days 0, 3, and 6 of the re-challenge period and again found that both groups still showed equivalent percentages of *S. epi*-specific Tregs in skin-draining LN (**Fig. 2.7J**). These results suggest that underlying systemic inflammation alone is not sufficient to influence commensal-specific $CD4^+$ T cell responses in skin and that there is a potential secondary role for the dissemination of live *S. epi*-2W during colitis or other colon-centric immune mechanisms that are not recapitulated with the LPS model, even in the presence of circulating microbial antigen.

2.2.3 Colitis, but not systemic inflammation, alters the intestinal $CD4^+$ T cell responses to *S. epidermidis*

Although most notably a human skin commensal bacterium, *S. epidermidis* has a less widely appreciated niche within the neonatal intestine (Adlerberth et al., 2006). Indeed, we found that *S. epi*-2W can stably colonize the colon even 11 days post-neonatal skin colonization in WT pups and can induce a substantial $2W^+$ $CD4^+$ T cell population in the colon lamina propria (LP) and gut-draining LN (**Fig. 2.8A and Fig. 2.8C**). Upon secondary skin challenge during adulthood, *S. epi*-2W was significantly more abundant in the colon-sourced stool of DSS-treated mice compared to controls (**Fig. 2.8C**), suggesting its differential ability to colonize in a perturbed gut environment.

Based on these observations, we sought to determine whether the breakdown of established antigen-specific tolerance to *S. epidermidis* originates in the gut. Using the same experimental setup (**Fig. 2.1A**), we looked at T cell responses in colon LP and gut-draining LN of DSS-treated mice compared to controls. Development of disease in

the acute DSS model is not T cell-dependent (Wirtz et al., 2017) but we found that polyclonal $CD4^+$ T cells accumulate in colon LP (**Fig. 2.8D**) and gut-draining LN (**Fig. 2.8F**) of DSS-treated mice by the end of the 10-day treatment period. $CD4^+$ T cell expansion combined with increased exposure to *S. epidermidis* in the gut resulted in significantly greater numbers of $2W^+CD44^+$ $CD4^+$ T cells in colon LP (**Fig. 2.8B and E**) and gut-draining LN (**Fig. 2.8B and G**) of DSS-treated mice compared to controls. As was evident in skin-draining LN and skin of DSS-treated mice, there was also a colitis-associated decrease in the percentage of *S. epi*-2W specific Tregs in gut-draining LN (**Fig. 2.8H**), but not in the polyclonal Treg population (**Fig. 2.8I**).

To understand the specificity of this response to colitis, we used our modified LPS sepsis model (**Fig. 2.7A**) to examine the intestinal *S. epi*-specific $CD4^+$ T cell response during systemic inflammation alone. Unlike the DSS-treated mice, there were no differences in the number of polyclonal (**Fig. 2.8J**) or $2W^+CD44^+$ $CD4^+$ T cells (**Fig. 2.8K**) nor in the quality of the response to *S. epi*-2W in gut-draining LN of LPS-injected mice, whether in an antigen-specific or polyclonal manner (**Fig. 2.8L and M**). These results suggest that DSS-induced colitis, but not LPS-induced sepsis, results in differential local responses to intestinal *S. epi*-2W.

Additionally, we asked whether intestinal colonization of *S. epi*-2W during colitis could result in alterations in the gut microbiota. To test this, we performed bacterial 16s rRNA sequencing on stool samples obtained from the colon of control and DSS-treated mice at day 10 of the *S. epi*-2W re-challenge period. In addition to significant changes in

microbial diversity (**Fig. 2.9A**) and notable differences in microbial composition (**Fig. 2.9B**), there were alterations in specific members of the community. Bacteria from the genus *Bacteroides* were substantially enriched in DSS-treated mice while those from the genus *Alloprevotella* were underrepresented (**Fig. 2.9C**). These results suggest that increased intestinal presence of *S. epi*-2W is not only directly leading to immune activation, but also influencing other potential host-microbe interactions through alterations in the surrounding microbial community.

To begin investigating the role of adult re-exposure to *S. epi*-2W in the altered antigen-specific $CD4^+$ T cell response, we performed two types of pilot experiments. In the former, we challenged WT mice in adulthood with *S. epi*-2W plus tape-stripping without prior neonatal colonization with *S. epi*-2W (**Fig. 2.10A**). There were no differences in either the antigen-specific or polyclonal Treg response in the skin-draining LN (**Fig. 2.10B and C**), indicating either the limitation of studying minimal antigen-specific Treg percentages in this model, which remains to be elucidated, or the importance of neonatal exposure and subsequent adult re-exposure to *S. epi*-2W. Intriguingly, this could mean that gut antigen-specific T cell populations, in conjunction with the intestinal *S. epi*-2W niche, aren't established in this adult-only context to elicit the potential mechanism of T cell trafficking, as will be discussed in the next section.

As a complementary approach, we tested whether re-exposure to the relevant antigen (2W) provided by a different commensal microbe (*Staphylococcus hominis*) would be sufficient in altering the cutaneous antigen-specific response. WT mice

colonized on postnatal days 7, 10, and 13 with *S. epi*-2W were alternatively re-challenged in adulthood with *S. hominis*-2W and tape-stripping during DSS treatment (**Fig. 2.11A**). Unlike what was seen upon re-challenge with *S. epi*-2W, there were no differences in the antigen-specific Treg response in the skin-draining and gut-draining LN upon re-challenge with a different commensal with the same 2W antigen (**Fig. 2.10B and C**), suggesting either a specific role for *S. epidermidis* pathogenesis during colitis or its re-expansion from neonatal seeding, both of which would largely not be possible without re-exposure to the same microbe.

2.2.4 Colitis enhances trafficking of intestinal T cells to the skin-draining LN during skin re-challenge with *S. epidermidis*

The increase with DSS in intestinal *S. epi*-specific $CD4^+$ T cells and their parallel skewing toward an effector rather than regulatory T cell response prompted us to examine the possibility that trafficking of $CD4^+$ cells from gut to skin might contribute to the altered cutaneous *S. epi-specific* response during colitis. To explore this possibility, we first sought to answer whether colitis led to accumulation in the skin-draining LN of $CD4^+$ T cells reactive to gut bacteria. For this, we employed an *in vitro* APC-T cell co-culture assay to measure antigen-specificity of skin-draining LN $CD4^+$ T cells for gut microbial antigens. $CD4^+$ T cells isolated from skin-draining LN of DSS-treated or control mice were labelled with cell trace dye and co-cultured with splenic antigen-presenting cells (APCs) pulsed with stool from DSS-treated WT SPF mice (**Fig. 2.12A**). After 48 hours their proliferation in response to these gut microbial antigens was assessed by using flow cytometry to measure tracer dye dilution. Strikingly, skin-

draining LN CD4$^+$ T cells from DSS-treated mice showed significantly increased proliferation in response to stool antigen as compared to donor cells from control mice (**Fig. 2.12B**). This difference was not elicited either in the absence of stool antigen or in response to the irrelevant antigen ovalbumin (OVA) (**Fig. 2.13A**), suggesting enhanced reactivity to gut microbes rather than non-specific cell proliferation.

As DSS-induced colitis results in an excess of systemically circulating gut microbial antigen (Eichele and Kharbanda, 2017), this result could reflect either migration of CD4$^+$ T cells from gut to skin-draining LN or local expansion in the skin-draining LN of gut-microbe responsive T cells. To more specifically test our hypothesis regarding CD4$^+$ T cell migration, we turned to an adoptive transfer model to measure the trafficking properties of intestinal CD4$^+$ T cells from DSS-treated vs. control mice. To generate and re-expand the intestinal *S. epi*-specific CD4$^+$ T cell compartment, WT donor mice were colonized as neonates with *S. epi*-2W and then re-challenged as adults with skin-tape stripping with or without DSS. Total CD4$^+$ T cells were then isolated from the gut-draining LN at day 7 post-DSS initiation and adoptively transferred i.p. into congenic Thy1.1 recipient mice that also received *S. epi*-2W colonization in conjunction with tape-stripping (**Fig. 2.12C**). To account for variable efficiency of each adoptive transfer, both skin-draining LN and spleen were harvested 48 hours post-transfer and the relative accumulation of intestinal CD4$^+$ T cells at these sites was measured by flow cytometry. Consistent with colitis inducing increased skin-homing capacity among gut-draining LN T cells, donor CD4$^+$ T cells from DSS-treated mice

showed increased accumulation in skin-draining LN over spleen compared to cells from healthy control donors (**Fig. 2.12D**).

Unfortunately, small numbers of 2W-specific $CD4^+$ T cells in our transferred polyclonal populations precluded us from assessing antigen-specificity in this experimental set-up. We therefore performed complementary adoptive transfer experiments using a newly engineered strain of *S. epidermidis* expressing the ovalbumin antigen (*S. epi*-OVA) and OT-II TCR-transgenic OVA-specific $CD4^+$ T cells. $CD45.1^+$ OT-II mice were pre-colonized with *S. epi*-OVA during the neonatal period and then re-colonized as adults along with skin tape-stripping. On day 7 post-challenge, total OT-II $CD4^+$ T cells were isolated from the gut-draining LN of DSS-treated or control OT-II mice and adoptively transferred via intraperitoneal injection into *S. epi*-OVA naïve $CD45.2^+$ WT recipients. Recipients then received *S. epi*-OVA skin colonization and tape-stripping in tandem with DSS-induced colitis to recapitulate the inflammatory environment in which these T cells would reside. Here, we extended the post-transfer period to 1 week before harvesting skin-draining LN and spleen to allow for maximal antigen exposure and compared trafficking (**Fig. 2.12E**). Intriguingly in this model, we also found that $CD4^+$ T cells from DSS-treated OT-II donors showed increased recruitment to skin-draining LN over spleen compared to $CD4^+$ T cells from control OT-II donors (**Fig. 2.12F**). These results suggest that colitis can induce differential trafficking properties among bacteria-specific $CD4^+$ T cells in the presence of persisting colitis-driven signals.

Next, to more directly test whether trafficking occurs from gut to skin in our model, we monitored the movement of endogenous immune cells *in vivo* using transgenic mice which express the green-to-red photoconvertible protein Kikume Green (KikGr). Upon exposure to near-UV light (436 nm), the fluorescence of photoconverted KikGr cells changes from green to red. No immunomodulatory effects have been reported in the KikGr photoconversion model (Nowotschin and Hadjantonakis, 2009), allowing us to use this technique on mice during DSS-induced colitis and skin bacterial challenge. To trace movement of intestinal $CD4^+$ T cells to the skin-draining LN, we performed laparotomy and photoconversion of the externalized intestines and gut-draining LN in DSS or control SPF mice on day 6 of *S. epi*-2W skin re-challenge. We confirmed that photoconversion of $CD45^+$ cells in this set-up was indeed limited to the intestinal tract by verifying the presence of $KikRed^+$ cells in gut-draining LN but not spleen or skin-draining LN 30 minutes post light exposure (**Fig. 2.13B**). Skin-draining LN, skin, gut-draining LN, small intestinal and colonic LP (**Fig. 2.13C**), and spleen were harvested 24 hours later and the number of photoconverted cells was enumerated at each site (**Fig. 2.12G**). Absolute numbers of trafficked $KikRed^+$ $CD45^+$ cells in the skin-draining LN of DSS versus control mice were not increased, and possibly reduced, at this early timepoint (**Fig. 2.13D**). However, when we measured the propensity for gut to skin cell trafficking among individual cell subsets by calculating the ratio of $KikRed^+$ cells in the skin-draining LN compared to those in the gut-draining LN, we found enrichment of gut-derived T cells, especially $CD4^+$ T cells, but not $CD11c^+MHCII^+$ antigen-presenting cells in the skin-draining LN of DSS-treated mice (**Fig. 2.12H**). This enrichment of gut-derived $CD4^+$ T cells was not seen in the spleen (**Fig. 2.12I**),

supporting the notion that colitis preferentially induces direct trafficking of $CD4^+$ T cells from gut to skin-draining LN during concurrent skin challenge with commensal bacteria.

As these results supported trafficking of $CD4^+$ T cells during colitis, we then proceeded to ask whether blocking lymphocyte circulation during the challenge phase of our model would alter quality of the *S. epi*-2W response in the skin-draining LN. To answer this, we transiently blocked lymphocyte egress from secondary lymphoid organs in our model by using the sphingosine-1-phosphate receptor antagonist, FTY720 (Matloubian et al., 2004). WT mice were pre-colonized with *S. epi*-2W during the neonatal period, then split into three groups. One group of mice was given water and injected i.p. with PBS, another group was given DSS and injected with PBS, and a third group was given DSS and injected with FTY720 (**Fig. 2.12J**). As in previous experiments (**Fig. 2.4A**), DSS-treated mice had a decreased percentage of Tregs among *S. epi*-2W specific cells in the skin-draining LN compared to controls. However, FTY720 treatment during the 10-day re-challenge period reverted this phenotype to a 2W+ Treg percentage comparable to controls (**Fig. 2.12K**). An accompanying increase in the percentage of polyclonal Tregs in the skin-draining LN of FTY720 and DSS-treated mice was also seen, possibly reflecting restricted movement of other non-2W-specific microbe-specific T cells (**Fig. 2.12L**). Cumulatively, these experiments support a central role for colitis-induced gut-to-skin trafficking of $CD4^+$ T cells in the altered response to skin commensal bacteria.

2.2.5 Colitis-driven IL-1R1 signaling on CD4+ T cells alters antigen-specific tolerance to *S. epidermidis*

Having identified that trafficking of $CD4^+$ T cells from gut to skin contributes to colitis-induced alteration in the cutaneous response to *S. epi*-2W, we next sought to understand the molecular mechanisms that underlie skewing of this commensal-specific response towards effector $CD4^+$ T cells and away from Tregs. Based on literature implicating IL-1α and IL-1β in pathogenesis of DSS-induced colitis and human IBD (Ligumsky et al., 1990) as well as in neutrophilic dermatoses (Marzano et al., 2019), we chose to explore the role of these two members of the IL-1 cytokine family in our model.

As anticipated, levels of IL-1β were increased significantly in the serum and modestly in the skin of DSS-treated mice during active colitis and concurrent skin challenge (**Fig. 2.14A and B**). In parallel, there was only a modest increase in serum and tissue levels of IL-1α in DSS-treated vs. control mice (**Fig. 2.14C**). This result, in conjunction with our prior work showing that IL-1β reduces the percentage of commensal-specific Tregs generated following neonatal skin colonization (Leech et al., 2019), led us to postulate that these colitis-induced cytokines were involved in skewing the response to *S. epi*-2W in the colon, and by extension the skin. Due to the importance of IL-1 signaling in initiating gut inflammation via myeloid cell activation, we opted to forgo experiments in *Il1r1*$^{-/-}$ mice which have been shown to demonstrate altered disease severity during DSS-induced colitis (González-Navajas et al., 2010). Instead, we focused our investigation on *Il1r1*$^{fl/fl}$ *CD4-Cre*$^{Tg+}$ mice in which IL-1 signaling

is deleted specifically in αβ T cells, a cell type dispensable for development of acute DSS-induced colitis.

Given that previous work has shown a T cell-intrinsic role for IL-1 signaling in $CD4^+$ T cell expansion, Th17 differentiation (Basu et al., 2015; Chung et al., 2009), and "licensing" of effector function (Ben Sasson et al., 2009; Jain et al., 2018) we hypothesized that excess IL-1α and IL-1β during colitis was skewing the commensal-specific $CD4^+$ response towards an effector rather than Treg phenotype. To test this, we colonized *Il1r1*$^{fl/fl}$ *Cd4-Cre*$^{Tg+}$ *(Cre*$^+$*)* and *Il1r1*$^{fl/fl}$ *Cd4-Cre*$^{Tg-}$ *(Cre*$^-$*)* littermates with *S. epi*-2W during neonatal life before re-challenging them as adults with *S. epi*-2W plus tape-stripping either with or without concurrent DSS-induced colitis (**Fig. 2.14D**). In the absence of colitis, where IL-1α and IL-1β levels were low, *Cre*$^+$ and *Cre*$^-$ mice demonstrated equivalent percentages of commensal-specific Tregs in the skin-draining LN, which were comparable to that seen in WT control mice. In contrast, during DSS-induced colitis the percentage of *S. epi*-2W Tregs was rescued in *Cre*$^+$ mice but remained low in *Cre*$^-$ controls (**Fig. 2.14E**). This restored commensal-specific Treg percentage in *Cre*$^+$ mice was accompanied by reduced absolute numbers of 2W-specific effector $CD4^+$ T cells in the skin-draining LN (**Fig. 2.14F**), whereas numbers of 2W-specfic Tregs were equivalent between the two groups (**Fig. 2.14G**). Notably, these differences in Treg percentage and effector T cell numbers did not extend to the polyclonal $CD4^+$ population in the skin-draining LN (**Fig. 2.14H-J**). Importantly, abrogated IL-1R signaling in $CD4^+$ T cells also reverted the increase IL-$17A^+$ $CD4^+$ T cell and neutrophil populations in skin normally seen in our DSS colitis model (**Fig.**

2.14K-L). These results suggest that IL-1 signaling in $CD4^+$ T cells, stimulated by colitis-precipitated elevations in circulating IL-1α and IL-1β levels, plays a role in expanding commensal-specific T effectors which then alters the gut and skin immune responses to *S. epi*-2W during colitis.

Mild skin injury through tape-stripping induces increased expression of pro-inflammatory cytokines such as IL-6 and IL-17A (Gregorio et al., 2010). To further characterize additional signals that are modulating the cutaneous immune response *S. epi*-2W during colitis, we tested whether the method of re-challenge could be playing a role. Neonatally-colonized WT mice were re-challenged with *S. epi*-2W either with or without tape-stripping during DSS treatment. Unexpectedly, DSS-treated mice which received skin colonization with *S. epi*-2W in the absence of tape-stripping failed to skew the antigen-specific Treg response, mimicking the phenotype of tape-stripped control mice (**Fig. 2.15A**) while the polyclonal response remained unchanged (**Fig. 2.15B**). Although these results warrant further investigation, they suggest the potential role of mild skin injury in eliciting local signals in the skin that enhance the ability of colitis-driven inflammation to influence a distal tissue. In addition to enhanced production of IL-1 proteins in our model, we also saw increased levels of IL-6, CXCL1, and IL-7 in serum and skin tissues of DSS-treated mice (**Fig. 2.16A-C**), suggesting the presence of other immune signaling pathways that could be contributing to our findings.

2.2.6 Corroborating evidence for the influence of intestinal inflammation and altered microbial communities on skin T cell responses

Although we were able to show the mechanisms by which intestinal inflammation could alter established immunity to a specific skin microbe, there remains the question of whether similar findings could be observed in a broader setting. Gnotobiotic mice are an excellent tool for studying the direct contribution of specific microbes in immune responses, as evidenced by the striking increase in cutaneous IL-17A producing γδ T cells upon mono-colonization with the skin commensal *Corynebacterium accolens* (Ridaura et al., 2018).

Since our own study was limited to the use of specific pathogen-free (SPF) mice, we sought out ongoing experiments where we could further investigate the extent of the "gut-skin axis". Fortunately, we were able to obtain skin samples from gnotobiotic mice undergoing intestinal colonization and DSS-induced inflammation in a now-published study (Nayak et al., 2021). Skin samples were harvested from two groups of germ-free mice that each received oral gavage of stool from either patient donor "M0" or donor "M1" and further separated into control and DSS-treated groups.

Although minimal skin colonization may occur in this setting as mice are constantly exposed to microbes in the cage environment, we found supporting evidence that intestinal-focused inflammation and differences in microbial composition result in a marked difference in skin immune responses. These responses seemed to be targeted, as we found differences in IL-13 and IL-17A-producing, but not IFNγ-producing, T cell populations. These differences in cytokine-producing T cell populations were more

pronounced when directly comparing control and DSS-treated groups (**Fig. 2.17**), highlighting the role of intestinal inflammation as a major driving force. These results provide corroborating evidence for the “gut-skin” phenomenon we observed, as there were differences in the cutaneous T cell response of gnotobiotic mice in a separate study focused on intestinal phenotypes and even devoid of additional skin perturbation.

DISCUSSION

Whereas previous work examining commensal-specific responses in the intestinal tract and skin have focused on these tissues separately, here, we provide evidence that intestinal inflammation can impact the quality of the adaptive immune responses to commensal bacteria in the skin. For mice in which adaptive immune tolerance to *S. epidermidis* had been established during infancy, DSS-induced colitis but not LPS-triggered sepsis resulted in reduced *S. epidermidis*-specific Tregs and increased skin inflammation during adulthood skin re-challenge. This phenomenon was accompanied and likely supported by the increased intestinal numbers of *S. epidermidis* and *S. epidermidis*-specific $CD4^+$ T cells during colitis, in tandem with colitis-induced extra-intestinal lymphocyte trafficking. Importantly, IL-1 signaling in T cells proved key to reducing the frequency of *S. epidermidis*-specific Tregs, providing evidence into how established immune responses to resident microbes can be disrupted in adulthood. Collectively, these results identify a context in which there is breakdown in the normal homeostatic compartmentalization of skin and gut host-microbe interactions and provide mechanistic insight into observed connections between inflammatory skin and intestinal disease.

It is established that host-microbe interactions in the intestinal tract can generate T cell pools that can contribute to inflammation in distal sites. For example, increased Th17 responses to intestinal microbes have been shown to facilitate pathology in models of autoimmune disease including arthritis, uveitis and nephritis (Wu et al. 2010, Horai et al. 2015, Krebs et al. 2016). While the three tissues affected in these studies—joint, eye, and kidneys—are not heavily-colonized by microbes, we examined the

connection between the intestinal tract and skin, which both harbor large and diverse microbial communities capable of influencing host immunity. The concept of linked gut and skin dysbiosis has been a topic of conjecture as relates to disease pathogenesis (De Pessemier et al. 2021; O'Neill et al., 2016; Salem et al., 2018). However, the few studies that have tackled the mechanistic connection between immunity at these two barrier sites have focused on anaphylaxis and allergy (Leyva-Castillo et al. 2019, Oyoshi et al. 2011, Rigoni et al. 2020). In contrast, our work emphasizes the role of intestinal-driven inflammation as a trigger for altered antigen-specific responses to skin bacteria.

Intestinal colonization by *S. epidermidis* and generation of a *S. epidermidis*-specific $CD4^+$ response in the colon were key features of our model. *S. epidermidis* is classically a commensal skin microbe in humans but can also colonize the infant intestinal tract as a founding member (Adlerberth et al. 2006) in part through breast milk seeding (Jiménez et al., 2008). Even though *S. epidermidis* is excluded from the gut with increasing age, its presence during a critical window of immune education may facilitate establishment a largely tolerogenic intestinal memory $CD4^+$ T cell pool (Knoop et al., 2018), matching that seen in skin (Scharschmidt et al., 2015). We found that intestinal levels of *S. epidermidis* increased during colitis, consistent with its ability to adapt and bloom under certain inflammatory conditions (Garcia-Gutierrez et al., 2020). The total burden of intestinal *S. epidermidis* was likely augmented in our model by the skin re-colonization we performed in parallel with DSS administration, and this may have further intensified the degree of $CD4^+$ clonal sharing between the two barrier sites.

Even so, these studies demonstrate the principle that overlap in microbial species or immune epitopes across barrier tissues in early life can support later immune-cross reactivity and, in the right context, inter-connected pathology.

The role for T cell trafficking from the intestinal tract in our model builds on other work demonstrating that systemic dissemination of intestinal T cells can augment immune-mediated disease at distant sites (Krebs et al., 2016; Morton et al., 2015). Although not yet fully defined, we suspect that the T cell trafficking we observed was the result of altered chemokine receptor expression re-directing intestinal-homing T cells to the skin, as has been shown previously in a mouse model of food allergy and skin inflammation (Oyoshi et al., 2011). Additionally, there remains the possibility that some degree of movement is antigen-dependent, i.e., that re-expanded, intestinal *S. epidermidis*-specific $CD4^+$ cells enter the circulation and are drawn specifically to skin-draining lymphoid tissue based upon recognition of cognate bacterial antigen. While of significant interest, these two possibilities remain challenging to fully disentangle.

Our findings also support the concept of contextual pathogenicity, i.e., that a combination of host and microbial factors impact the immunomodulatory properties of a given skin bacteria, such as *S. epidermidis* (Chen et al., 2018; Flowers and Grice, 2020). While normally viewed as a skin mutualist (Harrison et al., 2019; Lai et al, 2010), *S. epidermidis* can turn pathologic when it becomes bloodborne in an at-risk host. In specific situations, commensal bacteria can also elicit excessive inflammation even when in their preferred body niche. This has been well demonstrated for gut bacteria,

including *Bacteroides thetaiotaomicron* (Bloom et al., 2010), *Helicobacter hepaticus* (Chow et al., 2011; Xu et al., 2018), and *Prevotellaceae spp.* (Elinav et al., 2011), as well as to a lesser extent for skin strains (Gimblet et al., 2017; Kobayashi et al., 2015). In our model, several factors likely contributed to the altered, pro-inflammatory $CD4^+$ response to *S. epidermidis*, including breach of the intestinal barrier, increased *S. epidermidis* intestinal abundance during colitis and local disruption of skin homeostasis through tape-stripping. While studies looking for a role of the skin microbiome in disease have often focused on shifts in bacterial community composition that accompany flares (Byrd et al., 2018), our data emphasize that a change in the host immune response to a given microbe can be just as instrumental.

Fully elucidating the various factors that "flip" the immune response to resident skin bacteria will be important for understanding the full spectrum of microbiome-driven skin disease. Specific areas of immediate interest include IL-1β and related inflammasome pathways, which are already implicated in human IBD (Ligumsky et al., 1990), models of murine colitis (Arai et al., 1998; Elinav et al., 2011; McEntee et al., 2019; Seo et al., 2015), neutrophilic dermatoses (Lukens et al., 2013; Marzano et al., 2019) and a host of other skin disorders (Sá et al., 2016). In this study, we found IL-1β and to a lesser extent IL-1α increased in the skin as well as serum of *S. epidermidis*-challenged DSS-treated mice. The reduction in the percent of *S. epidermidis*-specific Tregs in tandem with an increase in IL-1β are reminiscent of our prior work demonstrating that this cytokine helps shape the differential responses to skin bacterial "friend" versus "foe" during neonatal priming (Leech et al., 2019). Here, we illustrate that

IL-1R1 signaling specifically on T cells is important for the altered commensal-specific response and that this pathway can play a role in tuning the quality of memory as well as the primary $CD4^+$ response. Like others (Harrison et al., 2019), we observed that *S. epidermidis*-specific $CD4^+$ Teffs are enriched for IL-17A production. Thus, T-cell intrinsic IL-1R1 signaling during colitis in our model likely serves to tip the balance away from Tregs in favor of Th17, either by promoting Th17 re-expansion or contributing to Treg instability and conversion.

Collectively, our results offer interesting implications for the etiology of neutrophilic dermatoses, especially those associated with underlying IBD. Although the role of innate immunity is well-established in these diseases, isolated targeting of IL-1R1 is only intermittently effective and usually T cell-directed therapies, such oral steroids, tumor-necrosis-factor-inhibitors or IL-12/IL-23 blockade, are required for disease control (Menghini et al., 2019). As we show here, this may reflect the involvement of commensal-specific T cells that contribute to skin pathology. While elective skin biopsy of neutrophilic dermatoses is challenging due to the concern for pathergy, any opportunity to examine shared clonality of skin and intestinal T cells in patients with IBD-driven disease would be of high interest to the field moving forward. Likewise, therapies aimed at specifically correcting commensal-specific T cell responses at either barrier site represent an avenue for future therapeutic research and development.

ACKNOWLEDGEMENTS

We want to thank James Moon for contribution of tetramer reagents and expertise, Michael Rosenblum, Ari Molofsky, John Leech, Jarish Cohen, and Joshua Moreau for helpful discussions, Susan Lynch and Clifford Lowell for helpful discussions and critical review of the manuscript, Jun Ma for training on the DSS colitis model, Feng Chun Liu (with support from Mark Looney and the UCSF Bakar ImmunoX Initiative) for training on mouse surgery, Marcela Taruselli for assistance with surgeries, Margaret Alexander and Renuka Nayak for training on intestinal tissue preparation, Michelle Chu for cloning of the *S. epi*-OVA strain, Yongmei Hu for mouse husbandry, Sepideh Nozzari for mouse genotyping and other technical lab support, and Preston Tasoff and Connie Ha (with support from the UCSF Microbial Genomics CoLab Incubator) for assistance with microbial sequencing. Flow cytometry data were generated in the UCSF Parnassus Flow Cytometry Core, which is supported by the Diabetes Research Center (DRC) grant, NIH P30 DK063720. This work was primarily funded by G.R.M. grants: UCSF BMS T32GM008568, NIGMS and National Science Foundation GRFP 1650113 and T.C.S. grants: NIH DP2AI144968 and Burroughs Wellcome Fund CAMS-1015631.

FIGURES

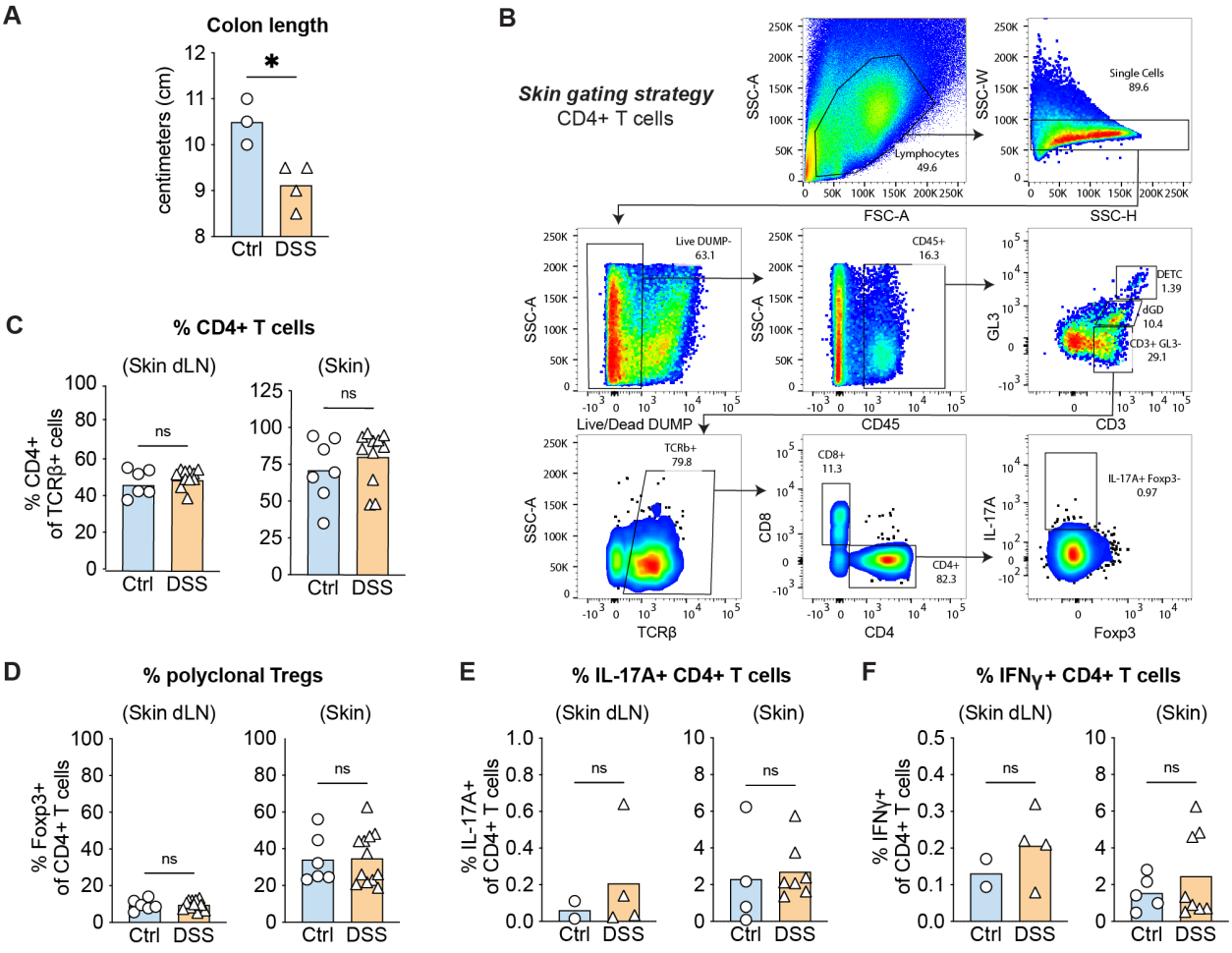

Figure 2.1. Acute intestinal inflammation alone does not alter the cutaneous T cell response.

A. Reduced colon length as a feature of disease in the DSS colitis model without skin re-challenge with *S. epi*-2W in the context of superficial skin abrasion (tape-stripping).
B. Gating strategy for IL-17A$^+$Foxp3$^-$CD4$^+$ T cells in skin.
C. Percentage of Foxp3$^+$ T cells as gated on CD4$^+$CD8$^-$ T cells in skin dLN and skin.
D. Percentage of CD4$^+$ T cells as gated on TCRβ$^+$ in skin dLN and skin.
E. Percentage of IL-17A$^+$ cells as gated on Foxp3$^-$CD4$^+$ T cells in skin dLN and skin.
F. Percentage of IFNγ$^+$ cells as gated on Foxp3$^-$CD4$^+$ T cells in skin dLN and skin.

Each point represents an individual mouse. All data above are representative of two independent experiments with at least two mice per group. P values correlate with symbols as follows: ns = not significant, p > 0.05, * p ≤ 0.05, ** p ≤ 0.01, *** p ≤ 0.001, **** p ≤ 0.0001.

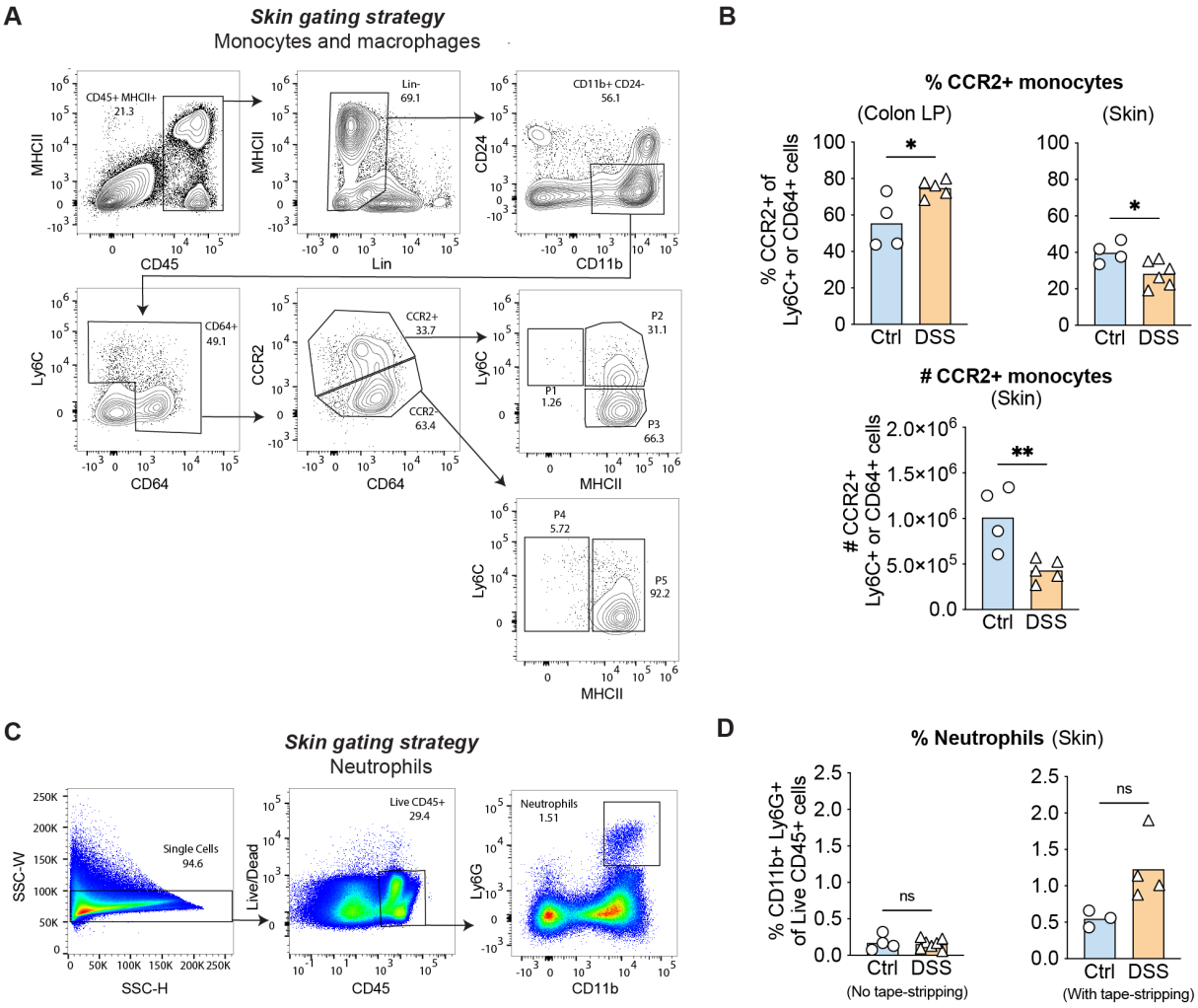

Figure 2.2. Mild skin injury enhances minimal alterations in the cutaneous myeloid response during acute colitis.

A. Gating strategy for different monocyte and macrophage subsets from Live CD45$^+$ cells in skin of DSS-treated mice without skin re-challenge with *S. epi*-2W and tape-stripping3.

B. Percentage and absolute numbers of skin CCR2$^+$ monocytes gated on Ly6C$^+$ and CD64$^+$ cells from colon LP and skin.

C. Percentage of CD11b$^+$ Ly6G$^+$ cells gated on Live CD45$^+$ in skin without tape-stripping and *S. epi*-2W re-challenge (left) or with tape-stripping, but without skin *S. epi*-2W re-challenge (right).

Each point represents an individual mouse. All data above are representative of one to two independent experiments with at least two mice per group. P values correlate with symbols as follows: ns = not significant, p > 0.05, * p ≤ 0.05, ** p ≤ 0.01, *** p ≤ 0.001, **** p ≤ 0.0001.

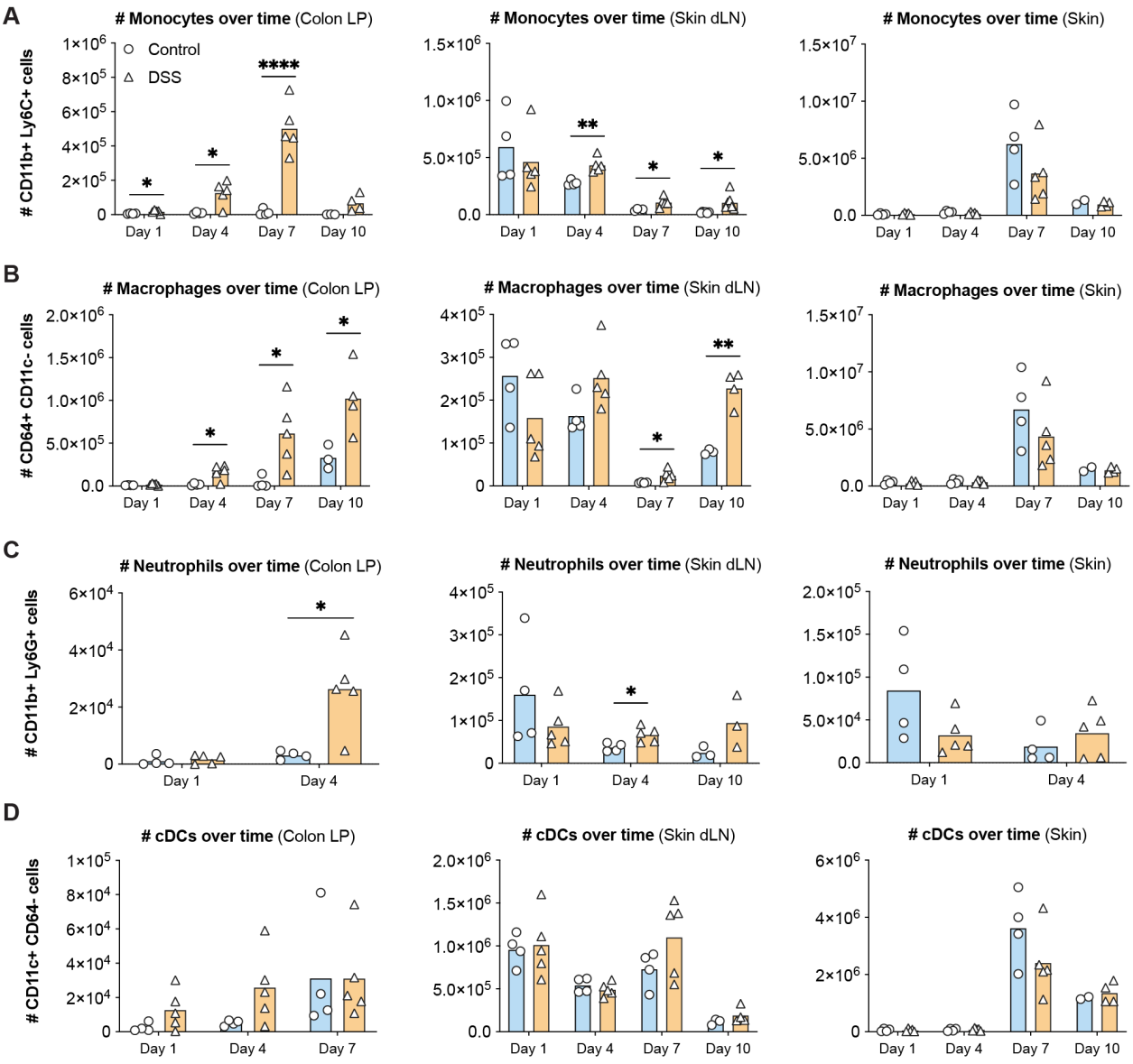

Figure 2.3. Intestinal inflammation and skin re-challenge with *S. epidermidis* alters the intestinal and skin-draining LN myeloid compartments.

A. Absolute numbers of $CD11b^{+}Ly6C^{+}$ monocytes in colon LP, skin dLN, and skin of control or DSS-treated mice during skin re-challenge with *S. epi*-2W in the context of superficial skin abrasion (tape-stripping).

B. Absolute numbers of $CD64^{+}CD11c^{-}$ macrophages in the same tissues as above.

C. Absolute numbers of $CD11b^{+}Ly6G^{+}$ neutrophils in colon LP, skin dLN, and skin of control or DSS-treated mice during skin re-challenge with *S. epi*-2W.

D. Absolute numbers of $CD11c^{+}CD64^{-}$ conventional DCs in colon LP, skin dLN, and skin of control or DSS-treated mice during skin re-challenge with *S. epi*-2W and tape-stripping.

Each point represents an individual mouse. All data above are representative of two independent experiments with at least two mice per group. P values correlate with symbols as follows: ns = not significant, $p > 0.05$, * $p \leq 0.05$, ** $p \leq 0.01$, *** $p \leq 0.001$, **** $p \leq 0.0001$.

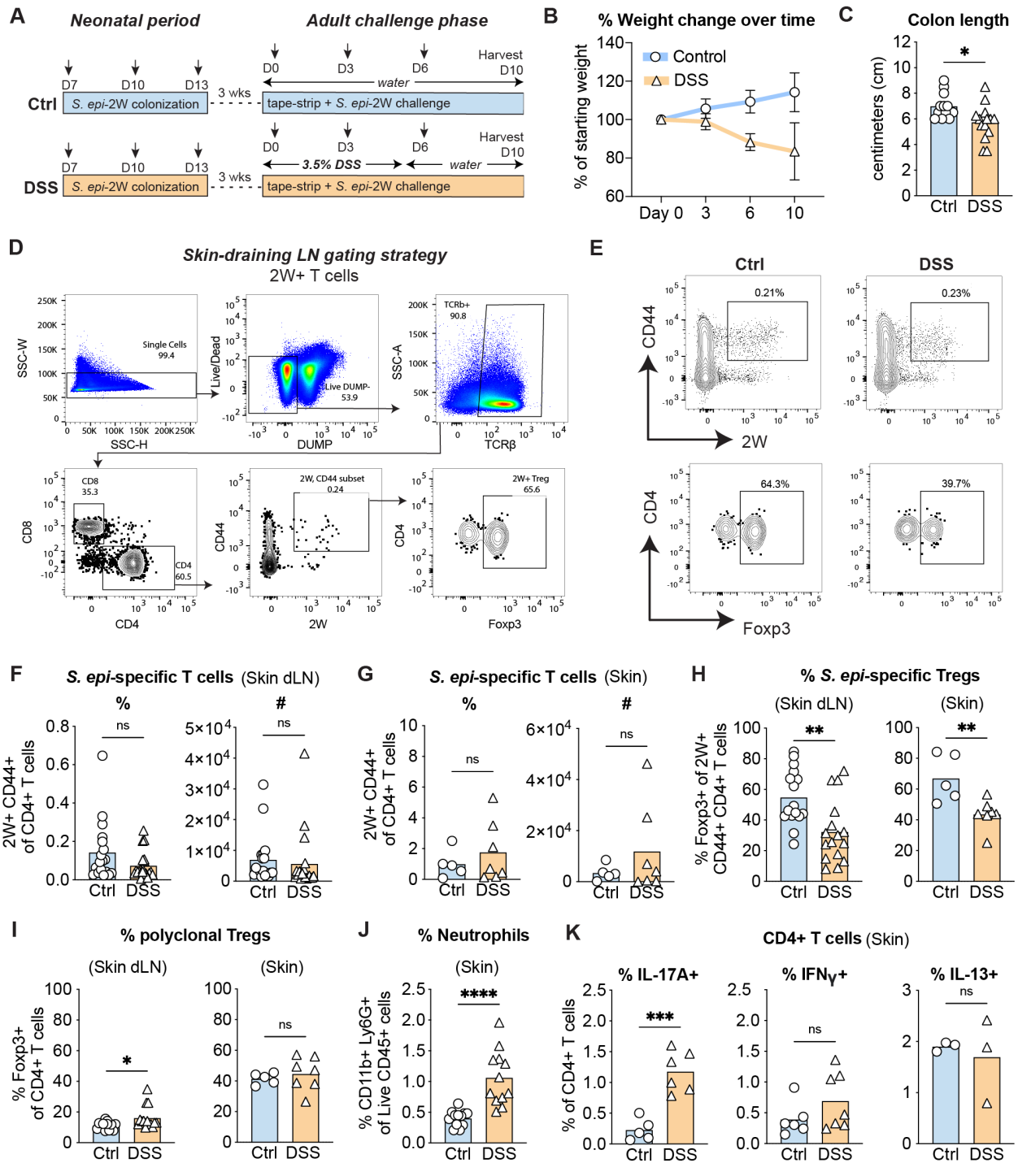

Figure 2.4. Acute intestinal inflammation alters the cutaneous immune response to *S. epidermidis*.

A. WT mice were colonized with *S. epi*-2W on postnatal days 7, 10, and 13 before induction of DSS colitis and skin re-challenge with *S. epi*-2W in the context of superficial skin abrasion (tape-stripping) three weeks later.

B. Increased weight loss as a feature of disease in the DSS colitis model.

C. Reduced colon length as a feature of disease in the DSS colitis model.

D. Gating strategy for Foxp3$^+$2W$^+$CD44$^+$CD4$^+$ T cells in skin dLN.

E. Representative flow cytometry plots of $2W^+CD44^+$ cells gated on Live $CD45^+DUMP^{neg}TCR\beta^+CD4^+$ from a tetramer-enriched fraction (top) and representative flow cytometry plots of $Foxp3^+$ cells gated on $2W^+CD44^+$ (bottom) in skin dLN from either control or DSS-treated mice on day 10 of the re-challenge phase.
F. Percentage (left) and absolute numbers (right) of $2W^+CD44^+CD4^+$ T cells in skin dLN.
G. Percentage (left) and absolute numbers (right) of $2W^+CD44^+CD4^+$ T cells in skin.
H. Percentage of $Foxp3^+2W^+CD44^+CD4^+$ T cells in skin dLN (left) and skin (right).
I. Percentage of $Foxp3^+CD4^+$ T cells in skin dLN (left) and skin (right).
J. Percentage of $Ly6G^+CD11b^+$ cells gated on live $CD45^+$ in skin.
K. Percentage of IL-$17A^+$, IFNγ^+, and IL-13^+ cells gated on Live $CD45^+CD3^+GL3^-TCR\beta^+CD4^+Foxp3^-$ in skin.

Each point represents an individual mouse. All data above are representative of two to four independent experiments with at least three mice per group. P values correlate with symbols as follows: ns = not significant, $p > 0.05$, * $p \leq 0.05$, ** $p \leq 0.01$, *** $p \leq 0.001$, **** $p \leq 0.0001$.

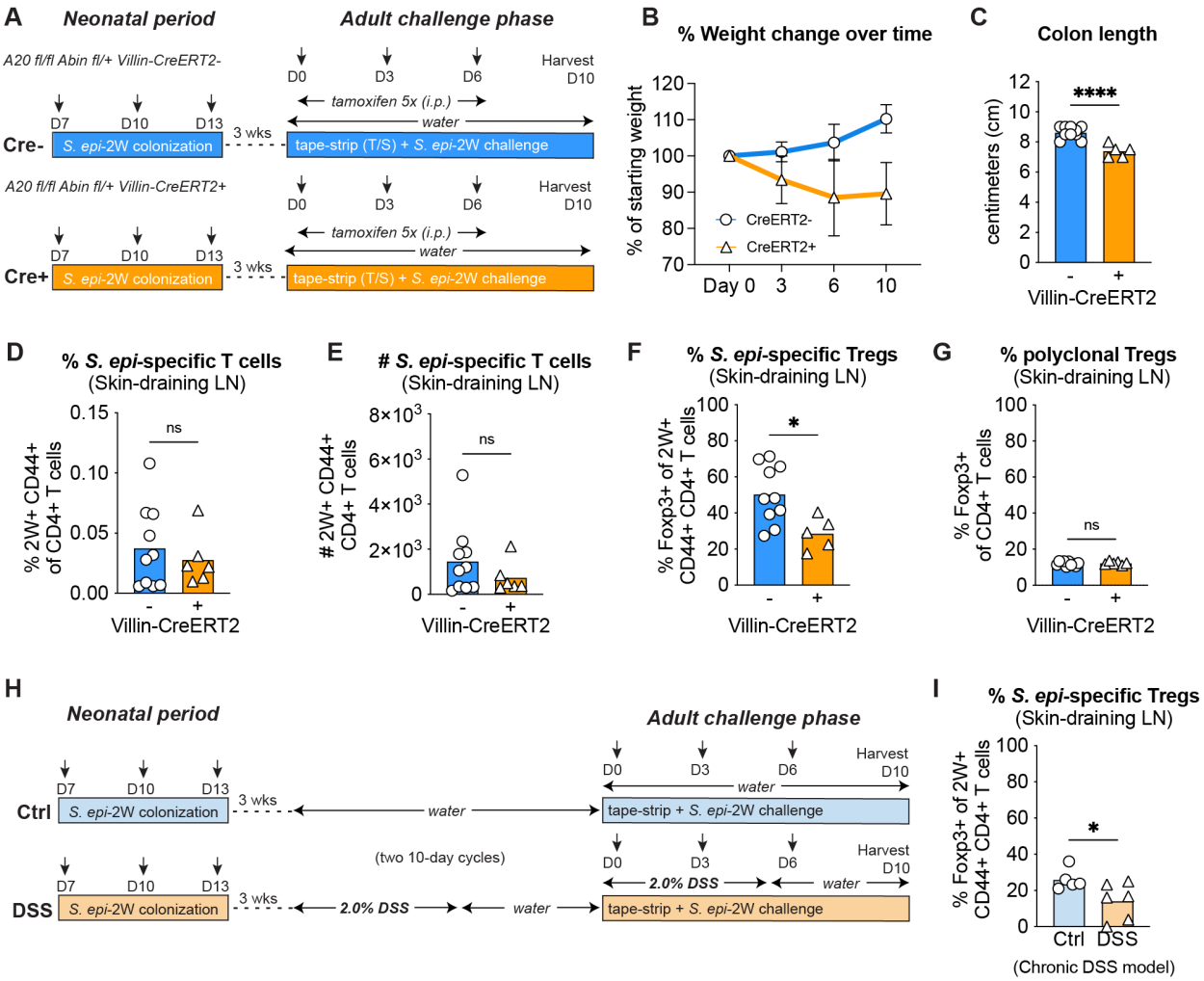

Figure 2.5. Alternative colitis models support the role of intestinal inflammation in altering the cutaneous antigen-specific CD4⁺ T cell response to *S. epidermidis*.

A. *Villin-Cre*⁺ and *Villin-Cre*⁻ mice were colonized with *S. epi*-2W on postnatal days 7, 10, and 13 before intraperitoneal tamoxifen injection and re-challenge with *S. epi*-2W in conjunction with tape-stripping three weeks later.
B. Increased weight loss as a feature of disease in the A20 ABIN-1 colitis model.
C. Reduced colon length as a feature of disease in the A20 ABIN-1 colitis model.
D. Percentage of 2W⁺CD44⁺CD4⁺ T cells in skin dLN.
E. Absolute numbers of 2W⁺CD44⁺CD4⁺ T cells in skin dLN.
F. Percentage of Foxp3⁺2W⁺CD44⁺CD4⁺ T cells in skin dLN.
G. Percentage of Foxp3⁺CD4⁺ T cells in skin dLN.
H. WT mice were colonized with *S. epi*-2W on postnatal days 7, 10, and 13 before induction of chronic DSS colitis for three weeks in adulthood. Skin re-challenge with *S. epi*-2W in the context of superficial skin abrasion (tape-stripping) was performed in the third and last 10-day cycle of DSS colitis.
I. Percentage of Foxp3⁺2W⁺CD44⁺CD4⁺ T cells in skin dLN.

Each point represents an individual mouse. All data above are representative of two to three independent experiments with at least two mice per group. P values correlate with symbols as follows: ns = not significant, $p > 0.05$, * $p \leq 0.05$, ** $p \leq 0.01$, *** $p \leq 0.001$, **** $p \leq 0.0001$.

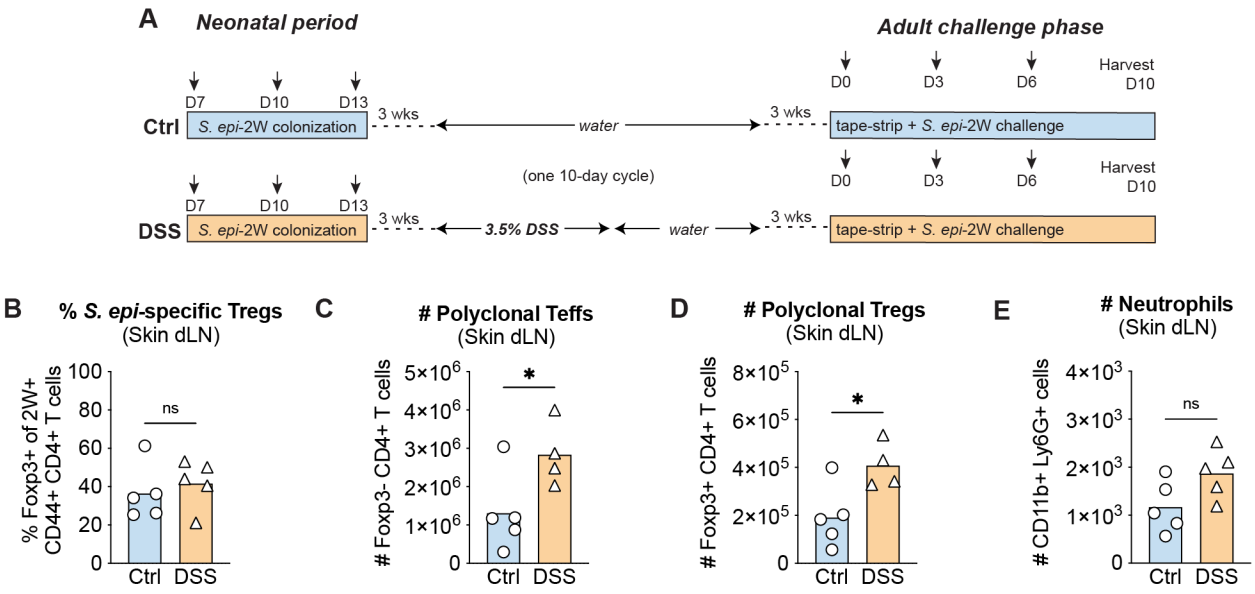

Figure 2.6. Prior acute intestinal inflammation has a persisting effect on T cell responses to subsequent skin re-challenge with *S. epidermidis*.

A. WT mice were colonized with *S. epi*-2W on postnatal days 7, 10, and 13 before induction of DSS colitis three weeks later. Skin re-challenge with *S. epi*-2W in the context of superficial skin abrasion (tape-stripping) was performed another three weeks post-colitis induction.
B. Percentage of $Foxp3^{+}2W^{+}CD44^{+}CD4^{+}$ T cells in skin dLN.
C. Absolute numbers of $Foxp3^{-}CD4^{+}$ T cells in skin dLN.
D. Absolute numbers of $Foxp3^{+}CD4^{+}$ T cells in skin dLN.
E. Absolute numbers of $Ly6G^{+}CD11b^{+}$ cells gated on live $CD45^{+}$ in skin dLN.

Each point represents an individual mouse. All data above are representative of one pilot experiment with at four to five mice per group. P values correlate with symbols as follows: ns = not significant, $p > 0.05$, * $p \leq 0.05$, ** $p \leq 0.01$, *** $p \leq 0.001$, **** $p \leq 0.0001$.

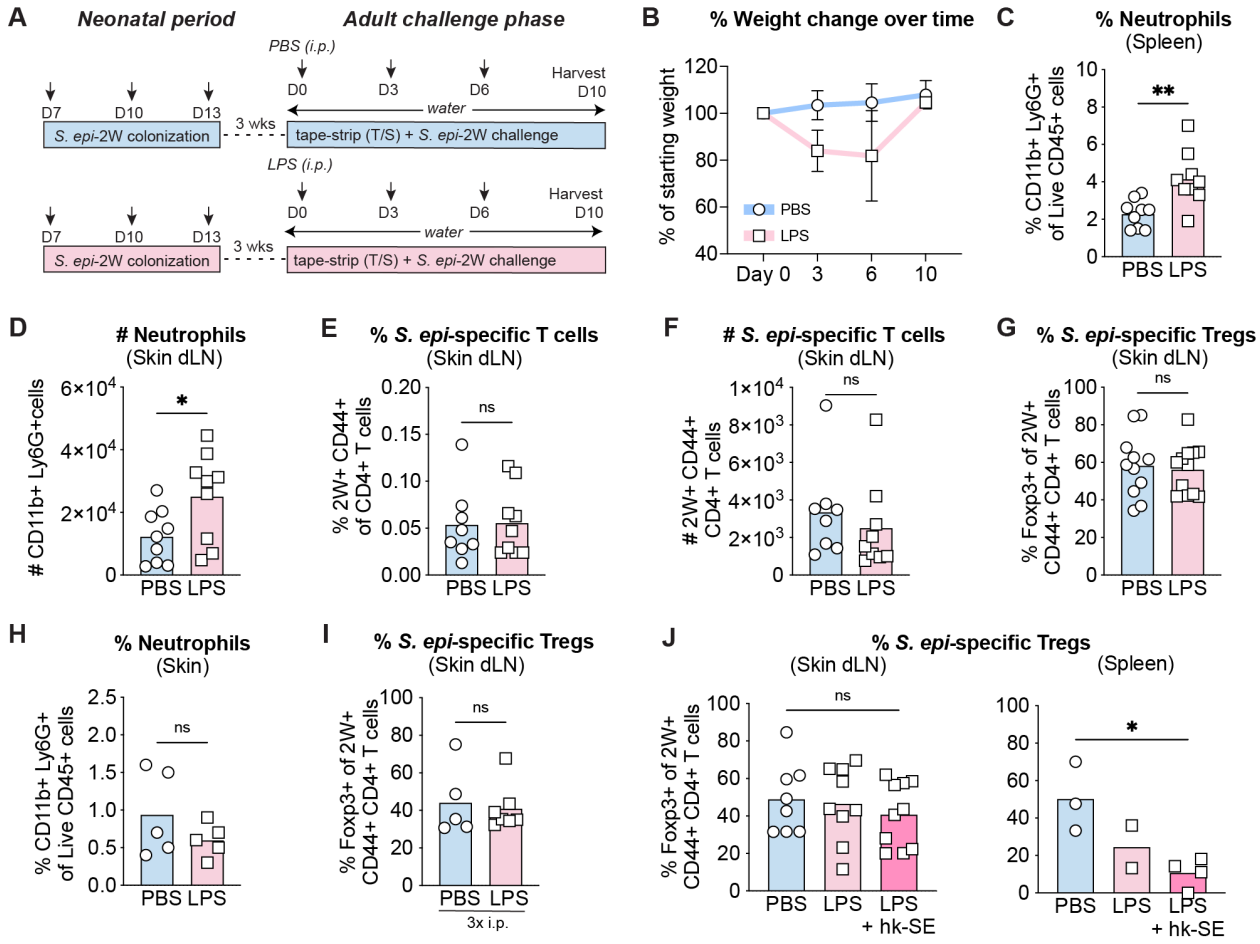

Figure 2.7. Acute systemic inflammation alone does not alter the cutaneous antigen-specific CD4+ T cell response to *S. epidermidis*.

A. WT mice were colonized with *S. epi*-2W on postnatal days 7, 10, and 13 before one i.p. injection with LPS (2 mg/kg) and re-challenge with *S. epi*-2W three weeks later.
B. Increased weight loss as a feature of disease in the LPS sepsis model.
C. Percentage of $Ly6G^+CD11b^+$ cells gated on Live $CD45^+$ in spleen.
D. Percentage of $Ly6G^+CD11b^+$ cells gated on Live $CD45^+$ in skin dLN.
E. Percentage of $2W^+CD44^+CD4^+$ T cells in skin dLN.
F. Absolute numbers of $2W^+CD44^+CD4^+$ T cells in skin dLN.
G. Percentage of $Foxp3^+2W^+CD44^+CD4^+$ T cells in skin dLN.
H. Percentage of $Ly6G^+CD11b^+$ cells gated on Live $CD45^+$ in skin.
I. Percentage of $Foxp3^+2W^+CD44^+CD4^+$ T cells in skin dLN in mice receiving three i.p. injections with LPS (1 mg/kg) and re-challenge with *S. epi*-2W.
J. Percentage of $Foxp3^+2W^+CD44^+CD4^+$ T cells in skin dLN (left) and spleen (right) in mice receiving three i.p. injections with LPS (1 mg/kg) mixed with heat-killed *S. epi*-2W during re-challenge with *S. epi*-2W.

Each point represents an individual mouse. All data above are representative of three independent experiments with two to three mice per group (except for spleen pilot in 2.7J). P values correlate with symbols as follows: ns = not significant, $p > 0.05$, * $p \leq 0.05$, ** $p \leq 0.01$, *** $p \leq 0.001$, **** $p \leq 0.0001$.

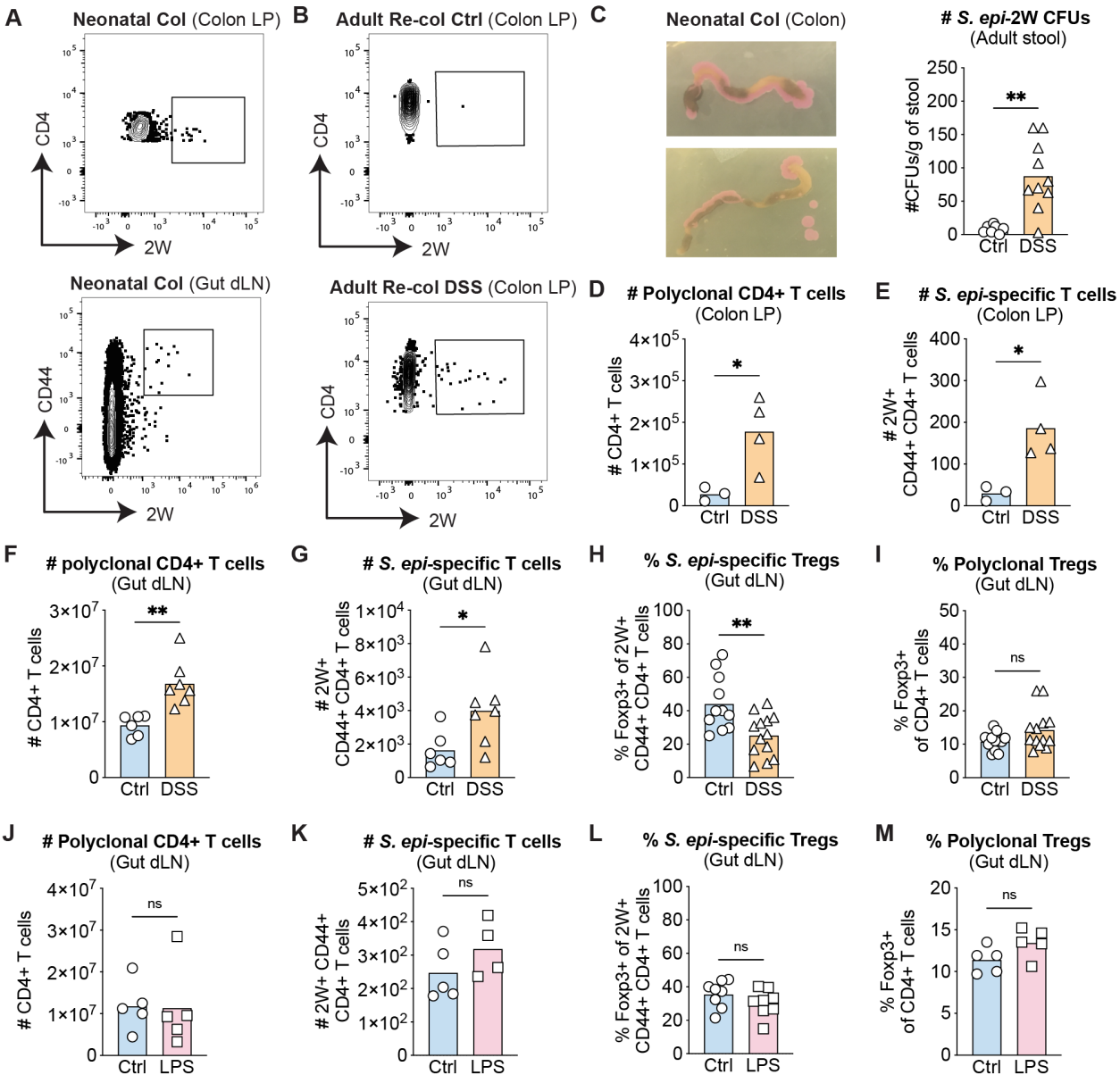

Figure 2.8. Acute intestinal inflammation, but not systemic inflammation, alters local colonization of and antigen-specific CD4⁺ T cell response to *S. epidermidis*.

A. Representative flow cytometry plots of 2W⁺CD44⁺ cells gated on Live CD45⁺CD3⁺GL3⁻TCRβ⁺CD4⁺ in colon lamina propria (LP) (top), or on Live CD45⁺DUMP^{neg}TCRβ⁺CD4⁺ in a tetramer-enriched fraction from gut dLN (bottom) of 24-day old mice colonized with *S. epi*-2W on postnatal days 7, 10, and 13.

B. Representative flow cytometry plots of 2W⁺CD44⁺ cells gated on Live CD45⁺CD3⁺GL3⁻TCRβ⁺CD4⁺ in colon lamina propria (LP) from either adult control (top) or DSS-treated mice (bottom) on day 10 of the re-challenge phase.

C. (Left) Representative sections of colon from 21-day old mice colonized with *S. epi*-2W on postnatal days 7, 10, and 13. Tissues were plated on TSA with erythromycin to show growth of *S. epi*-2W mCherry. (Right) Absolute numbers of colony forming units (CFUs) in stool obtained directly from colon of adult mice from control or DSS-treated groups.

D. Absolute numbers of CD4⁺ T cells in colon LP from control or DSS-treated groups.

E. Absolute numbers of 2W⁺CD44⁺CD4⁺ T cells in colon LP from control or DSS-treated groups.

F. Absolute numbers of CD4⁺ T cells in gut dLN from control or DSS-treated groups.

G. Absolute numbers of $2W^+CD44^+CD4^+$ T cells in gut dLN from control or DSS-treated groups.
H. Percentage of $Foxp3^+2W^+CD44^+CD4^+$ T cells in gut dLN from control or DSS-treated groups.
I. Percentage of $Foxp3^+CD4^+$ T cells in gut dLN from control or DSS-treated groups.
J. Absolute numbers of $CD4^+$ T cells in gut dLN from control or LPS-injected groups.
K. Absolute numbers of $2W^+CD44^+CD4^+$ T cells in gut dLN from control or LPS-injected groups.
L. Percentage of $Foxp3^+2W^+CD44^+CD4^+$ T cells in gut dLN from control or LPS-injected groups.
M. Percentage of $Foxp3^+CD4^+$ T cells in gut dLN from control or LPS-injected groups.

Each point represents an individual mouse. All data above are representative of at least two independent experiments with at two or three mice per group. P values correlate with symbols as follows: ns = not significant, $p > 0.05$, * $p \leq 0.05$, ** $p \leq 0.01$, *** $p \leq 0.001$, **** $p \leq 0.0001$.

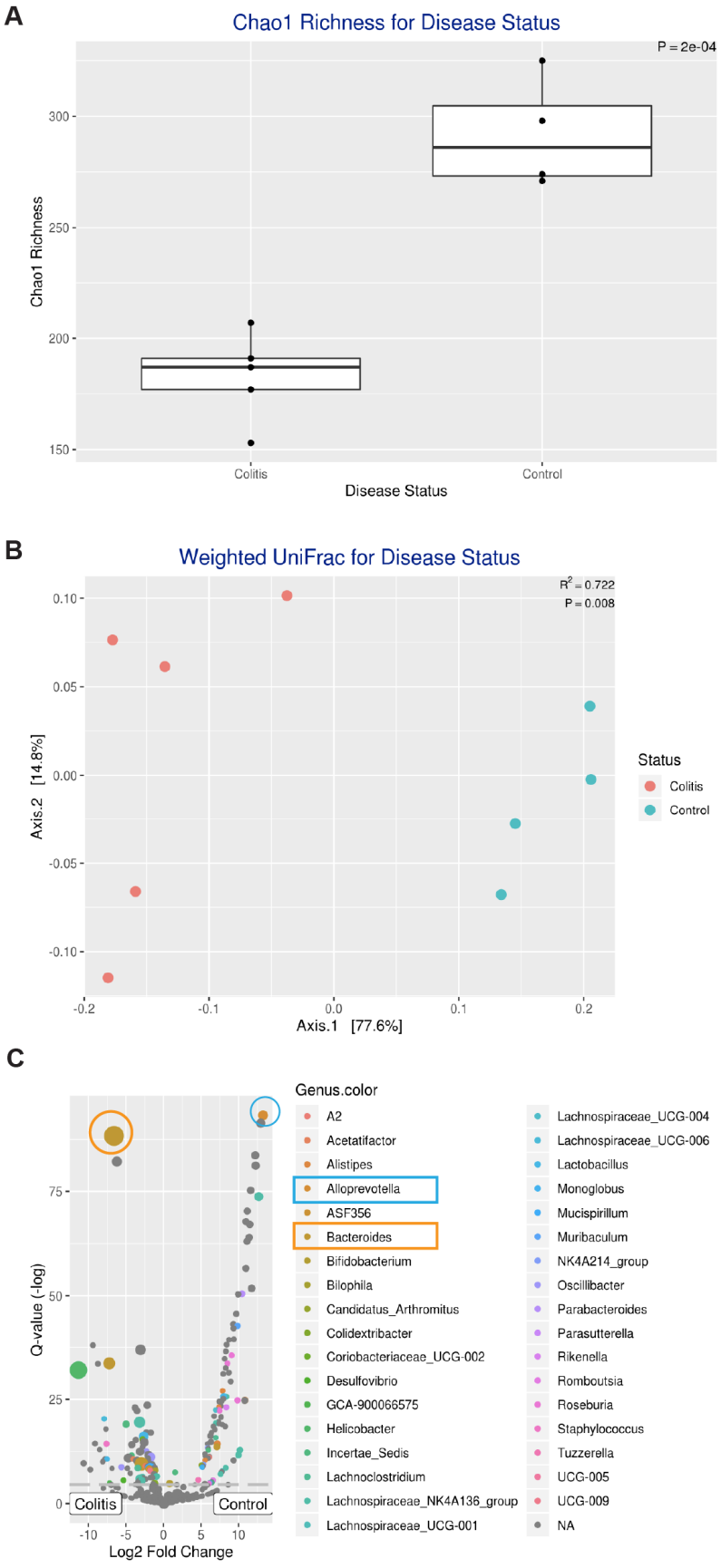
A
Chao1 Richness for Disease Status
P = 2e-04
Chao1 Richness
300
250
200
150
Colitis
Control
Disease Status
B
Weighted UniFrac for Disease Status
R2 = 0.722
P = 0.008
Axis.2 [14.8%]
0.10
0.05
0.00
-0.05
-0.10
-0.2
-0.1
0.0
0.1
0.2
Axis.1 [77.6%]
Status
Colitis
Control
C
Genus.color
Q-value (-log)
75
50
25
0
Colitis
Control
-10
-5
0
5
10
Log2 Fold Change
A2
Acetatifactor
Alistipes
Alloprevotella
ASF356
Bacteroides
Bifidobacterium
Bilophila
Candidatus_Arthromitus
Colidextribacter
Coriobacteriaceae_UCG-002
Desulfovibrio
GCA-900066575
Helicobacter
Incertae_Sedis
Lachnoclostridium
Lachnospiraceae_NK4A136_group
Lachnospiraceae_UCG-001
Lachnospiraceae_UCG-004
Lachnospiraceae_UCG-006
Lactobacillus
Monoglobus
Mucispirillum
Muribaculum
NK4A214_group
Oscillibacter
Parabacteroides
Parasutterella
Rikenella
Romboutsia
Roseburia
Staphylococcus
Tuzzerella
UCG-005
UCG-009
NA

Figure 2.9. Intestinal inflammation and skin re-challenge with *S. epidermidis* alters the composition of intestinal microbial communities.

A. Richness is the number of different taxa (greater richness equals more taxa). Analysis of Variance (ANOVA) comparison was performed using the richness measure as represented here and two other measures (equitability and phylogenetic diversity, not shown). Alpha-diversity for all three measures significantly varies between control and DSS (colitis) groups.
B. Permutational Analysis of Variance (PERMANOVA) was used on a variety of different distance matrices, including weighted (accounting for abundance of taxa) UniFrac, a measure of phylogenetic relatedness. The values in the R^2 column indicate the proportion of variance explained by the Disease Status, and the p-value indicates whether the comparison was statistically significant. If Disease Status explained a significant proportion of variance, a PCoA plot is produced. In this plot, each dot is a sample, and the distance between two samples is a reflection of their similarity. Samples closer together are more similar while samples further apart are compositionally more distinct. For Weighted UniFrac, PERMANOVA analysis found R^2 >70% of statistically significant variance in the microbiome due to disease status, as indicated by the r-squared value. The variance explained is significant ($p<0.01$).
C. Significant enrichment of OTUs was determined using DESeq2. Raw count data were normalized by accounting for effect size prior to differential abundance calculations based on the negative binomial Wald test; p-values were adjusted by using the Benjamini-Hochberg method for false discovery rate. (Highlighted in orange) Genus most significantly enriched in DSS colitis compared to control group: *Bacteroides*. (Highlighted in blue) Genus most significantly enriched in control compared to DSS colitis group: *Alloprevotella*.

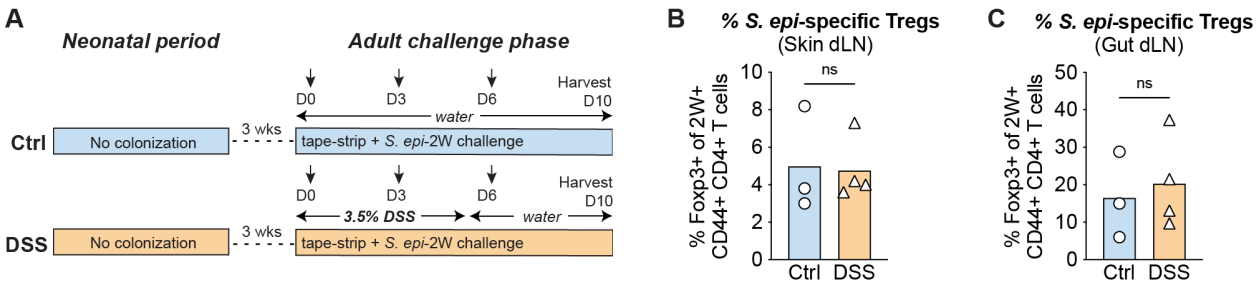

Figure 2.10. Altered response to *S. epidermidis* during colitis is dependent on neonatal colonization with *S. epidermidis*.

A. WT mice remained uncolonized with *S. epi*-2W postnatally. Induction of DSS colitis and skin re-challenge with *S. epi*-2W were performed three weeks later.
B. Percentage of $Foxp3^+2W^+CD44^+CD4^+$ T cells in skin dLN from control or DSS-treated mice.
C. Percentage of $Foxp3^+2W^+CD44^+CD4^+$ T cells in gut dLN from control or DSS-treated mice.

Each point represents an individual mouse. All data above are representative of one pilot experiment with three to four mice per group. P values correlate with symbols as follows: ns = not significant, $p > 0.05$, * $p \leq 0.05$, ** $p \leq 0.01$, *** $p \leq 0.001$, **** $p \leq 0.0001$.

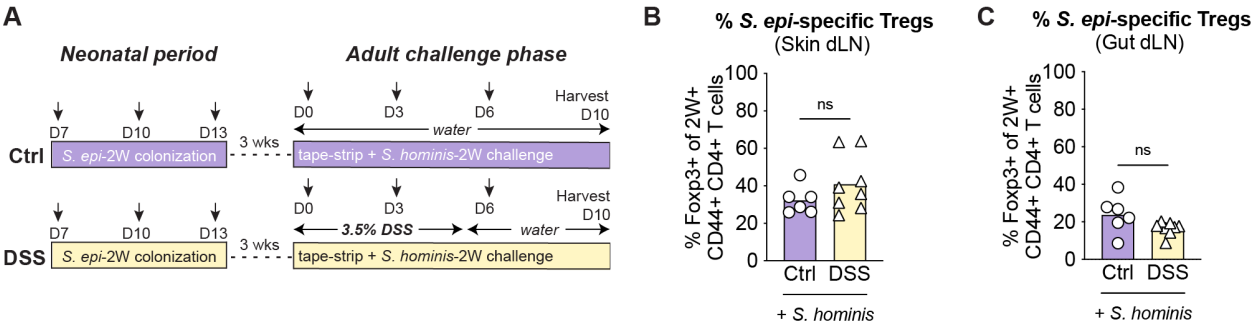

Figure 2.11. Re-challenge with another skin commensal, *S. hominis*, is not sufficient to alter the antigen-specific CD4+ T cell response during colitis.

A. WT mice were colonized with *S. epi*-2W on postnatal days 7, 10, and 13. Induction of DSS colitis and skin re-challenge with *S. hominis*-2W were performed three weeks later.
B. Percentage of Foxp3$^+$2W$^+$CD44$^+$CD4$^+$ T cells in skin dLN from control or DSS-treated mice.
C. Percentage of Foxp3$^+$2W$^+$CD44$^+$CD4$^+$ T cells in gut dLN from control or DSS-treated mice.

Each point represents an individual mouse. All data above are representative of two experiments with at least three mice per group. P values correlate with symbols as follows: ns = not significant, $p > 0.05$, * $p \leq 0.05$, ** $p \leq 0.01$, *** $p \leq 0.001$, **** $p \leq 0.0001$.

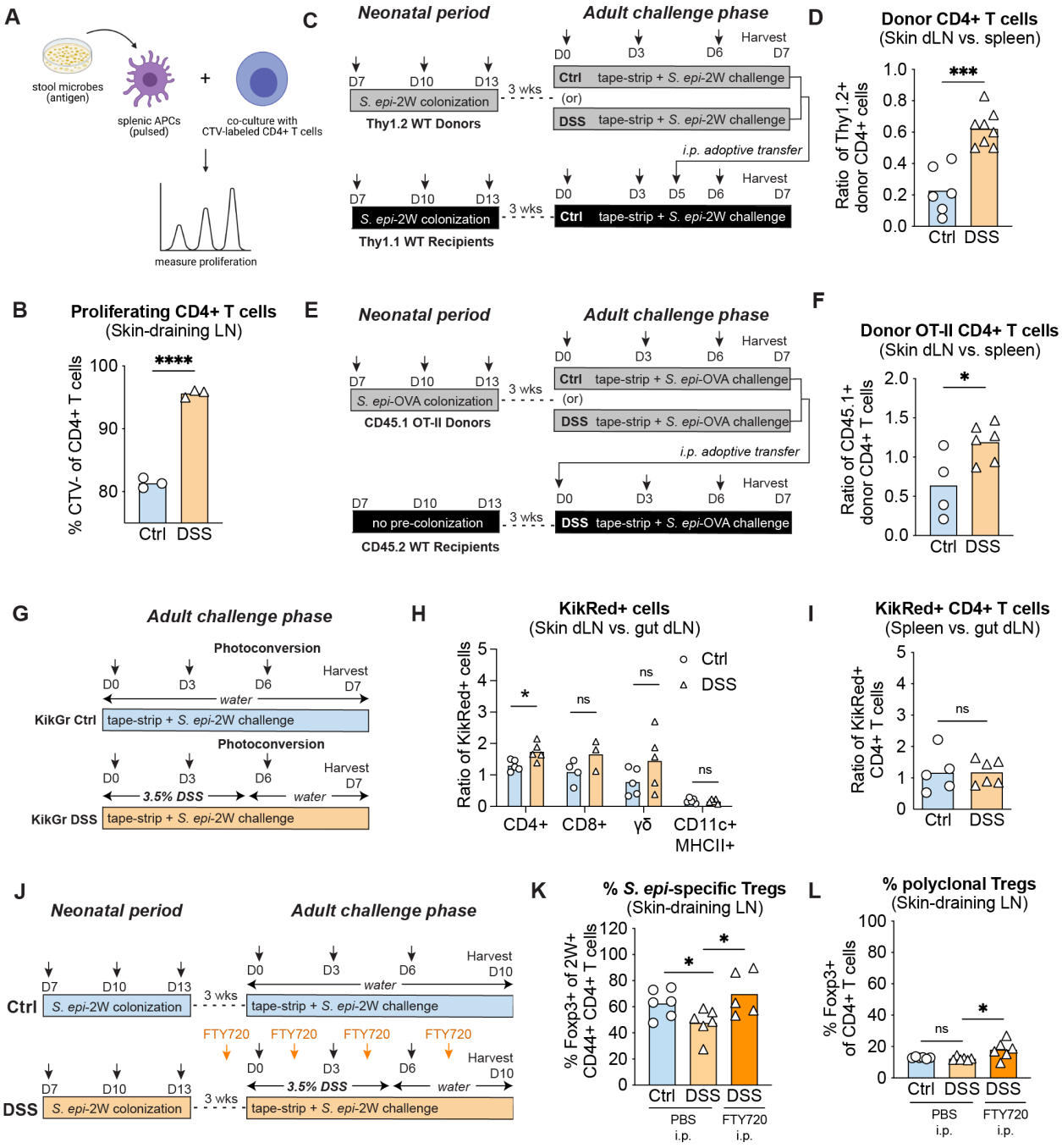

Figure 2.12. Acute intestinal inflammation alters trafficking of intestinal CD4+ T cells to skin-draining LN in response to *S. epidermidis* re-challenge.

A. Splenic antigen-presenting cells (APCs) were pulsed with stool and co-cultured with CellTrace™ Violet-labelled $CD4^+$ T cells from skin dLN of DSS-treated or control mice.

B. Proliferation was assessed by taking the CellTrace™ Violet negative population gated on live $CD45^+CD3^+GL3^-TCR\beta^+CD4^+$. Data is representative of one experiment with three individual mice per group.

C. Total $CD4^+$ T cells were obtained from gut dLN of either DSS-treated or control Thy1.2 mice at day 7 of the re-challenge phase, then adoptively transferred (i.p.) into Thy1.1 recipients undergoing the same re-challenge.

D. Ratio of $Thy1.2^+$ cells among Live $CD45^+CD3^+GL3^-TCR\beta^+CD4^+$ in skin dLN vs. in spleen.

E. Total $CD4^+$ T cells were obtained from gut dLN of either DSS-treated or control CD45.1 OT-II mice at day 7 of the re-challenge phase, then adoptively transferred (i.p.) into CD45.2 WT recipients undergoing primary skin challenge with *S. epi*-2W.
F. Ratio of $CD45.1^+$ cells among Live $CD45^+CD3^+GL3^-TCR\beta^+CD4^+$ cells in skin dLN vs. spleen. Each point represents an individual mouse. All data above are representative of one pilot experiment with three mice per group.
G. KikGr mice were colonized with *S. epi*-2W on postnatal days 7, 10, and 13 before induction of DSS colitis and re-challenge with *S. epi*-2W in the context of superficial skin abrasion three weeks later. At day 7 of the re-challenge phase, laparotomy and photoconversion of intestinal tissue were performed in both groups. Tissues were collected 24 hours post-photoconversion.
H. Ratio of $CD45^+$ cell subsets among $KikRed^+$ cells in skin dLN vs. among $KiKRed^+$ cells in gut dLN.
I. Ratio of $CD4^+$ cells among $KikRed^+$ cells in spleen vs. gut dLN. Each point represents an individual mouse.
J. WT mice were colonized with *S. epi*-2W on postnatal days 7, 10, and 13 before induction of DSS colitis and re-challenge with *S. epi*-2W in the context of superficial skin abrasion three weeks later. One group of DSS-treated mice received i.p. injections of FTY720 and another group received i.p. injections of PBS every other day during the re-challenge phase.
K. Percentage of $Foxp3^+2W^+CD44^+CD4^+$ T cells in skin dLN from control, DSS-treated and PBS-injected, and DSS-treated and FTY720-injected groups.
L. Percentage of $Foxp3^+CD4^+$ T cells in skin dLN from control, DSS-treated and PBS-injected, and DSS-treated and FTY720-injected groups.

Each point represents an individual mouse. All data from 2.12C-2.12L are representative of two to three independent experiments with at least two mice per group. P values correlate with symbols as follows: ns = not significant, $p > 0.05$, * $p \leq 0.05$, ** $p \leq 0.01$, *** $p \leq 0.001$, **** $p \leq 0.0001$.

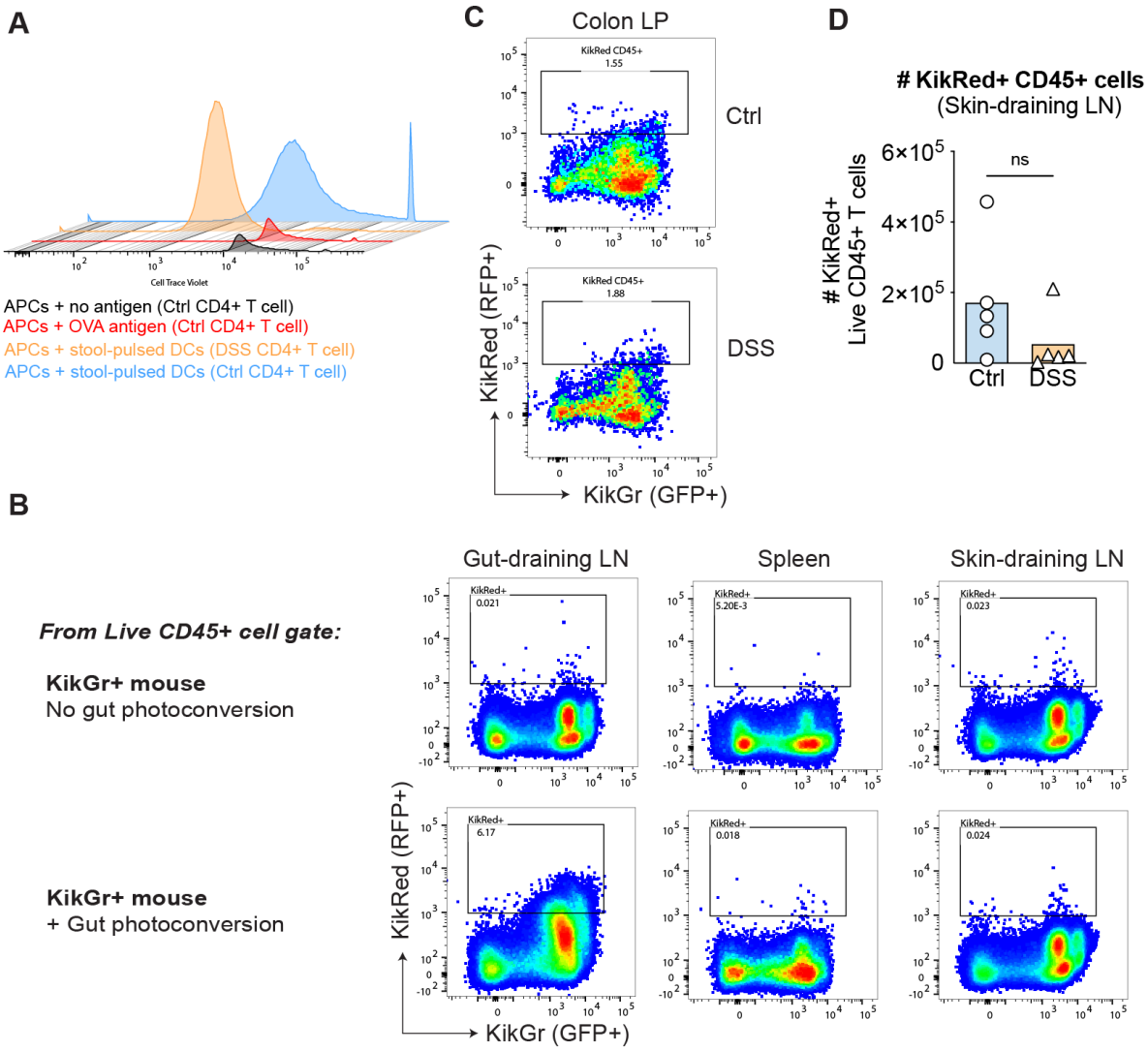

Figure 2.13. Gating strategies for *in vitro* and photoconversion experiments.

A. Representative histograms of CellTrace™ Violet-negative (proliferating) $CD4^+$ T cells in negative control samples (black and red) and test samples (blue and orange).

B. Representative flow cytometry plots of $KikRed^+$ (RFP^+) cells among Live $CD45^+$ in gut dLN, spleen, and skin dLN of $KikGr^+$ mice that were unexposed (top) vs. exposed to violet light (bottom).

C. Representative flow cytometry plots of $KikRed^+$ (RFP^+) cells among Live $CD45^+$ in colon LP.

D. Absolute numbers of $KikRed^+$ (RFP^+) Live $CD45^+$ cells in skin dLN in control or DSS-treated mice.

Each point represents an individual mouse. Data in 2.13D are representative of two independent experiments with at least two mice per group. P values correlate with symbols as follows: ns = not significant, $p > 0.05$, * $p \leq 0.05$, ** $p \leq 0.01$, *** $p \leq 0.001$, **** $p \leq 0.0001$.

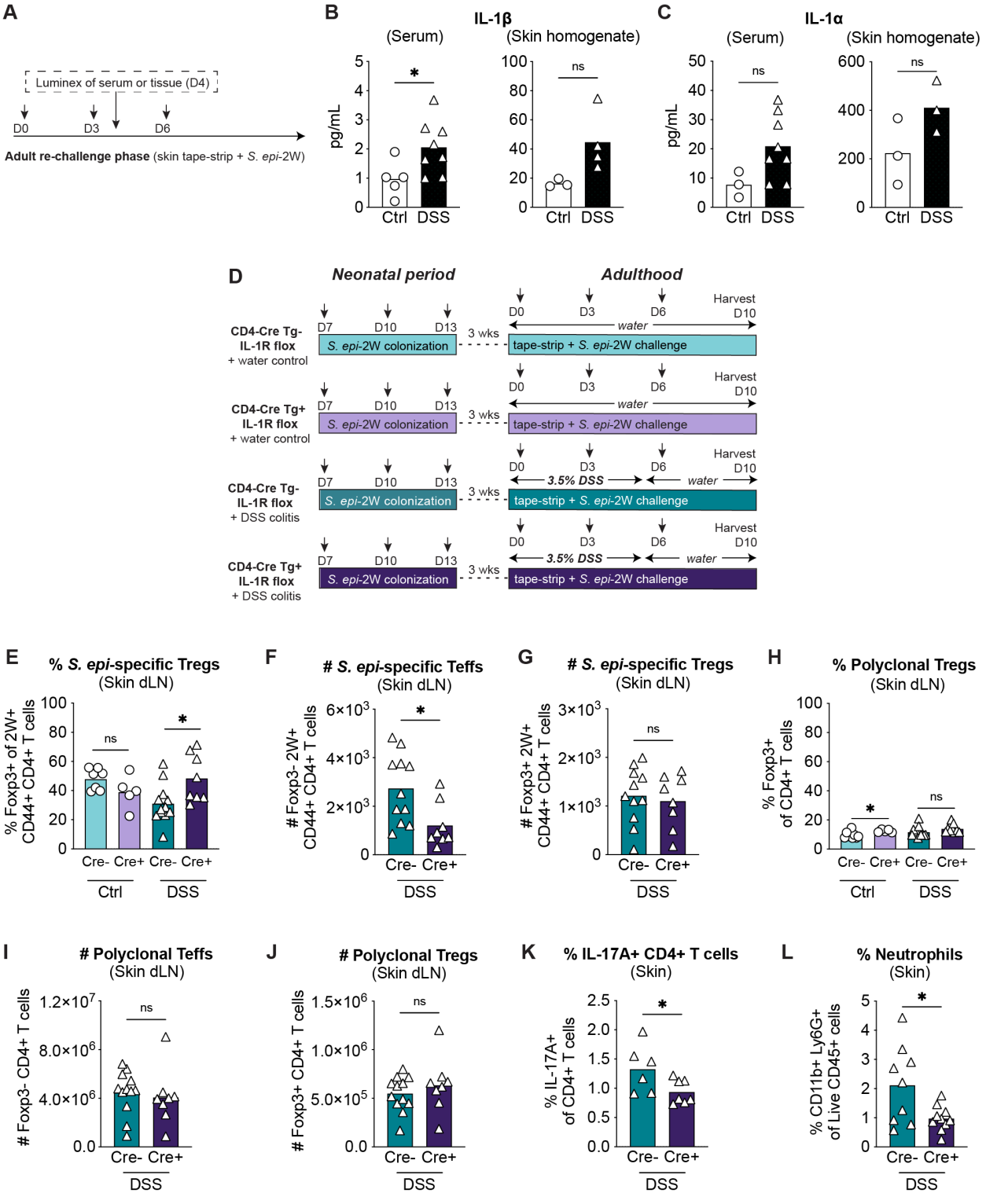
A
Luminex of serum or tissue (D4)
D0
D3
D6
Adult re-challenge phase (skin tape-strip + S. epi-2W)
B
IL-1β
(Serum)
(Skin homogenate)
pg/mL
Ctrl
DSS
ns
C
IL-1α
(Serum)
(Skin homogenate)
D
Neonatal period
Adulthood
CD4-Cre Tg- IL-1R flox + water control
CD4-Cre Tg+ IL-1R flox + water control
CD4-Cre Tg- IL-1R flox + DSS colitis
CD4-Cre Tg+ IL-1R flox + DSS colitis
D7
D10
D13
3 wks
S. epi-2W colonization
D0
D3
D6
Harvest D10
water
3.5% DSS
tape-strip + S. epi-2W challenge
E
% S. epi-specific Tregs
(Skin dLN)
% Foxp3+ of 2W+ CD44+ CD4+ T cells
Cre-
Cre+
F
S. epi-specific Teffs
(Skin dLN)
Foxp3- 2W+ CD44+ CD4+ T cells
G
S. epi-specific Tregs
(Skin dLN)
Foxp3+ 2W+ CD44+ CD4+ T cells
H
% Polyclonal Tregs
(Skin dLN)
% Foxp3+ of CD4+ T cells
I
Polyclonal Teffs
(Skin dLN)
Foxp3- CD4+ T cells
J
Polyclonal Tregs
(Skin dLN)
Foxp3+ CD4+ T cells
K
% IL-17A+ CD4+ T cells
(Skin)
% IL-17A+ of CD4+ T cells
L
% Neutrophils
(Skin)
% CD11b+ Ly6G+ of Live CD45+ cells

Figure 2.14. Colitis-driven IL-1 signaling to $CD4^+$ T cells skews the cutaneous immune response to *S. epidermidis.*

A. On day 4 of the re-challenge phase, serum and skin tissue were collected from control or DSS-treated WT mice re-challenged with *S. epi*-2W. Samples were analyzed for IL-1 proteins via multiplexed ELISA.
B. Concentration of IL-1β from serum and skin homogenates of control or DSS-treated mice on day 4 of the re-challenge period.
C. Concentration of IL-1α from serum and skin homogenates of control or DSS-treated mice on day 4 of the re-challenge period.
D. *CD4-Cre*$^+$ and *CD4-Cre*$^-$ mice were colonized with *S. epi*-2W on postnatal days 7, 10, and 13 before DSS treatment and re-challenge with *S. epi*-2W three weeks later.
E. Percentage of $Foxp3^+2W^+CD44^+CD4^+$ T cells in skin dLN from *CD4-Cre*$^+$ and *CD4-Cre*$^-$ control or DSS-treated groups.
F. Absolute numbers of $Foxp3^-2W^+CD44^+CD4^+$ T cells in skin dLN from DSS-treated groups.
G. Absolute numbers of $Foxp3^+2W^+CD44^+CD4^+$ T cells in skin dLN from DSS-treated groups.
H. Percentage of $Foxp3^+CD4^+$ T cells in skin dLN from control or DSS-treated groups.
I. Absolute numbers of $Foxp3^-CD4^+$ T cells in skin dLN from control or DSS-treated groups.
J. Absolute numbers of $Foxp3^+CD4^+$ T cells in skin dLN from control or DSS-treated groups.
K. Percentage of IL-$17A^+$ cells gated on Live $CD45^+CD3^+GL3^-TCR\beta^+CD4^+Foxp3^-$ in skin.
L. Percentage of $Ly6G^+CD11b^+$ cells gated on live $CD45^+$ in skin.

Each point represents an individual mouse. All data above are representative of three to four independent experiments with at least three mice per group. P values correlate with symbols as follows: ns = not significant, $p > 0.05$, * $p \leq 0.05$, ** $p \leq 0.01$, *** $p \leq 0.001$, **** $p \leq 0.0001$.

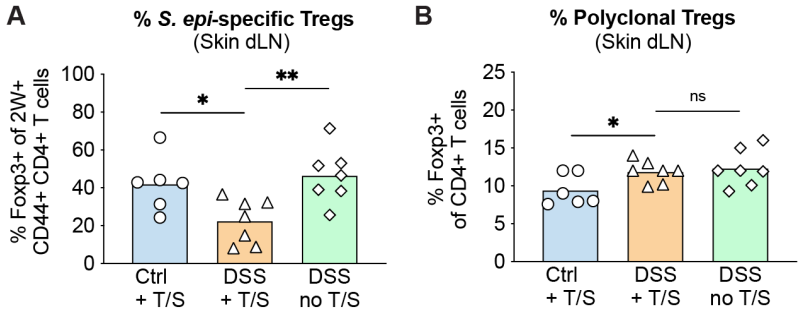

Figure 2.15. Mild skin injury is indispensable for inducing the altered cutaneous response to *S. epidermidis* during colitis.

WT mice were colonized with *S. epi*-2W on postnatal days 7, 10, and 13. Induction of DSS colitis and skin re-challenge with *S. epi*-2W, either with or without tape-stripping, were performed three weeks later.

A. Percentage of $Foxp3^+2W^+CD44^+CD4^+$ T cells in skin dLN from control or DSS-treated mice.

B. Percentage of $Foxp3^+CD4^+$ T cells in skin dLN from control or DSS-treated mice.

Each point represents an individual mouse. All data above are representative of two experiments with at least three mice per group. P values correlate with symbols as follows: ns = not significant, $p > 0.05$, * $p \leq 0.05$, ** $p \leq 0.01$, *** $p \leq 0.001$, **** $p \leq 0.0001$.

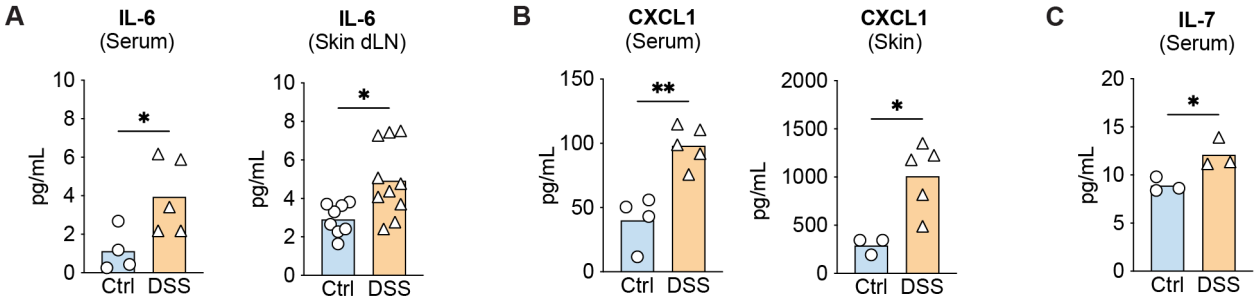

Figure 2.16. Acute intestinal inflammation drives production of other cytokines and chemokines that can skew the T cell response during re-challenge with *S. epidermidis*.

A. On day 4 of the re-challenge phase, serum and skin dLN homogenates were collected from control or DSS-treated WT mice re-challenged with *S. epi*-2W. Samples were analyzed for cytokines and chemokines via multiplexed ELISA.
B. Concentration of IL-6 from serum and skin dLN homogenates of control or DSS-treated mice.
C. Concentration of CXCL1 from serum and skin dLN homogenates of control or DSS-treated mice.
D. Concentration of IL-7 from serum of control or DSS-treated mice.

Each point represents an individual mouse. All data above are representative of two independent experiments with at least two mice per group. P values correlate with symbols as follows: ns = not significant, $p > 0.05$, * $p \leq 0.05$, ** $p \leq 0.01$, *** $p \leq 0.001$, **** $p \leq 0.0001$.

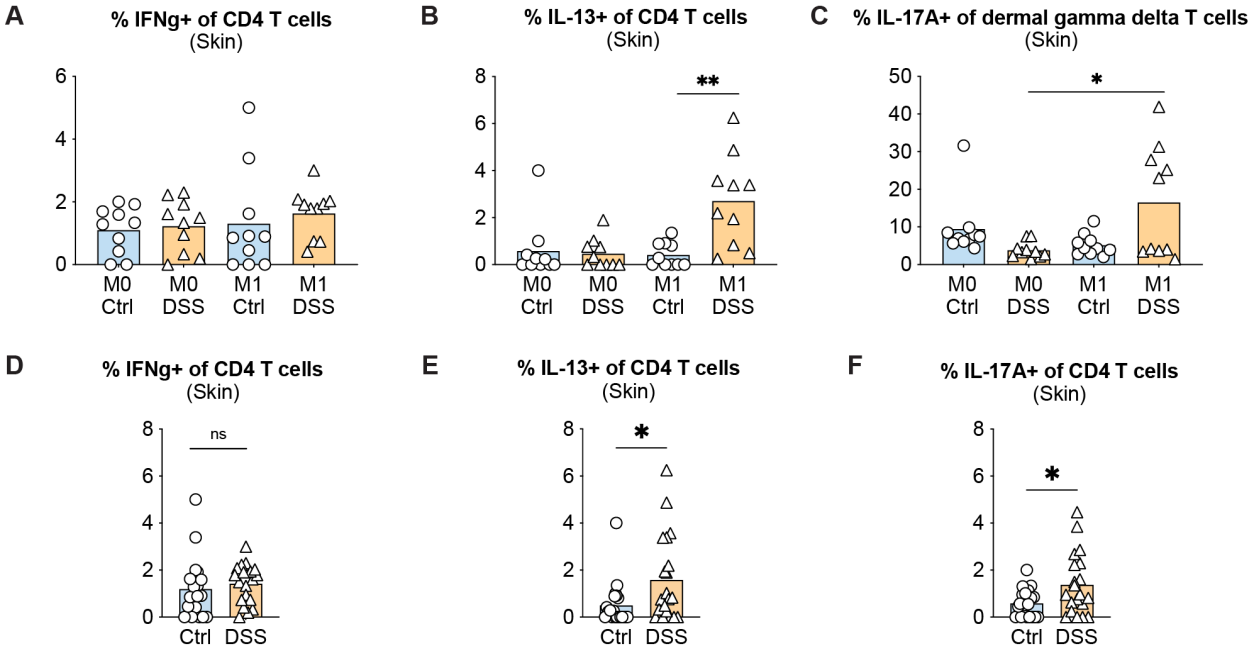

Figure 2.17. Corroborating evidence for the influence of intestinal inflammation and microbial dysbiosis on skin T cell responses.

A. Percentage of IFNγ^{+} cells gated on Live CD45^{+}CD3^{+}GL3^{-}TCRβ^{+}CD4^{+}Foxp3^{-} in skin. Gnotobiotic mice are separated into groups by patient stool donor (M0 or M1) and experimental treatment.
B. Percentage of IL-13^{+} cells gated on Live CD45^{+}CD3^{+}GL3^{-}TCRβ^{+}CD4^{+}Foxp3^{-} in skin. Gnotobiotic mice are separated into groups by patient stool donor (M0 or M1) and experimental treatment.
C. Percentage of IL-17A^{+} cells gated on Live CD45^{+}CD3^{+}GL3^{+} in skin. Gnotobiotic mice are separated into groups by patient stool donor (M0 or M1) and experimental treatment.
D. Percentage of IFNγ^{+} cells gated on Live CD45^{+}CD3^{+}GL3^{-}TCRβ^{+}CD4^{+}Foxp3^{-} in skin. Gnotobiotic mice are separated into groups by experimental treatment.
E. Percentage of IL-13^{+} cells gated on Live CD45^{+}CD3^{+}GL3^{-}TCRβ^{+}CD4^{+}Foxp3^{-} in skin. Gnotobiotic mice are separated into groups by experimental treatment.
F. Percentage of IL-17A^{+} cells gated on Live CD45^{+}CD3^{+}GL3^{-}TCRβ^{+}CD4^{+}Foxp3^{-} in skin. Gnotobiotic mice are separated into groups by experimental treatment.

Each point represents an individual mouse. All data above are representative of two independent experiments with at least five mice per group. P values correlate with symbols as follows: ns = not significant, $p > 0.05$, * $p \leq 0.05$, ** $p \leq 0.01$, *** $p \leq 0.001$, **** $p \leq 0.0001$.

CHAPTER 3: MATERIALS AND METHODS

Experimental Model and Subject Details

Experimental Animals

Wild-type C57BL/6 mice were originally purchased from Jackson Laboratories (Bar Harbor, ME), then bred and maintained in the UCSF specific pathogen-free (SPF) facility on the Parnassus campus for use in experiments. *Il1r*$^{fl/fl}$, *Cd4-Cre,* and *CAG::KikGr* (Kitamoto et al., 2020) mice were purchased from Jackson and bred in-house. *A20*$^{fl/fl}$*, Abin*$^{fl/fl}$*,* and *Villin-Cre*^{ERT2} mice were a gift from A. Ma. All animals were 7 days to 10 weeks old at the time of experiments. Littermates of the same sex were socially housed under a 12 h light/dark cycle and randomly assigned to experimental groups whenever possible. Animal work was performed in accordance with the NIH Guide for the Care and Use of Laboratory Animals and the guidelines of the Laboratory Animal Resource Center and Institutional Animal Care and Use Committee of the University of California, San Francisco.

Bacterial Strains and Culture Conditions

Staphylococcus epidermidis (*S. epi*) strain Tü3298 (Allgaier et al., 1986; Augustin and Götz, 1990) was used in this study and grown in tryptic soy broth at 37ºC. Bacterial media was supplemented with 5 mg/mL erythromycin for plasmid selection. In current and published work, *S. epi* has been engineered to express the 2W model antigen linked to the fluorophore mCherry under control of the *agr* promoter via plasmid pJL74-2W-gpmCherry (Leech et al., 2019). In this work, the same Tü3298 strain was engineered to express the OVA peptide antigen via modification of the original pJL74-2W-gpmCherry plasmid.

Method Details

Colitis Models

5 to 6-week old wild-type C57BL/6 mice were given 2.5-3.5% DSS (w/v) (Alfa Aesar, Catalog No. 9011-18-1) *ad libitum* in their drinking water for 5-6 days, with one round of replacement on days 3 or 4. 5 to 6-week old $A20^{fl/fl}$ $Abin^{fl/+}$ $Villin\text{-}Cre^{ERT2\ Tg+}$ or $^{Tg-}$ mice were given daily intraperitoneal injections of 1 mg tamoxifen (1 mg/d, Catalog No. T5648; Sigma Aldrich) for 5 consecutive days. In both models, colon length was measured from end of the cecum to beginning of the rectum. Weight loss was calculated as a percentage of daily weight over starting weight.

FTY720 Administration

FTY720 (Selleck Chemicals, Catalog No. S5002) was dissolved in phosphate buffered saline (PBS) and administered to 5 to 6-week old wild-type C57BL/6 mice via intraperitoneal injection at a dose of 10 mg/kg as previously described (Scharschmidt et al., 2015). For experiments depicted in Figure 4, FTY720 was administered every 48 hours on re-challenge days 0-10. Control mice (littermates) were treated with equal volumes of PBS according to the same schedule.

LPS-induced Sepsis Model

Purified lipopolysaccharides (LPS) from Salmonella enterica serotype minnesota (Sigma, Catalog No. L6261) was dissolved in phosphate buffered saline (PBS) and administered to 5 to 6 week-old wild-type C57BL/6 mice via intraperitoneal injection at a dose of 2 mg/kg or 1 mg/kg on day 0 or on days 0, 3, and 6 of the re-challenge period.

Bacterial Skin Colonization and Light Skin Abrasion Models

S. *epi*-2W was cultured for 48 hours to achieve high 2W-mCherry expression as measured by flow cytometry, then washed and re-suspended in PBS to obtain 10^8-10^9 colony-forming units (CFUs) at a volume of 100 µL per mouse. S. *epi*-2W was then applied via a plastic pipette and a sterile PBS-soaked cotton-tipped swab to the back skin of mice on days 7, 10, and 13 for neonatal colonization.

To mimic physiologic exposure of mice to skin S. *epi*-2W in the context of light skin abrasion during adulthood, back hair was first removed using small animal clippers and depilatory cream (Nair™ Hair Remover Body Cream) on day 0, followed by repeated application and removal of adhesive tape on days 0, 3, and 6 (Shurtape HP-500). Tissues were harvested 10 days after initiation of the challenge as previously described (Scharschmidt et al., 2015).

APC-T cell In Vitro Assay

The APC-T cell assay using fecal samples was informed by previous work (Fujimura et al., 2016), with modifications specific to our model.

APCs: Spleens were harvested and processed over sterile 100 µM cell strainers in 1 mL of T cell media (RPMI supplemented with HyClone Characterized Fetal Bovine Serum (FBS), 1% penicillin-streptomycin, β-mercaptoethanol, HEPES and GlutaMAX™) before ACK lysis. Samples were then stained with Biotin anti-mouse CD3ε Antibody (BioLegend, clone 145-2C11, Catalog No. 100303) and Biotin anti-mouse/human CD45R/B220 Antibody (BioLegend, clone RA3-6B2, Catalog No. 103203) and APCs

were isolated using the EasySep™ Mouse Streptavidin RapidSpheres™ Isolation Kit (Catalog No. 19860).

Antigen: Stool contents obtained directly from harvested colon were homogenized in pre-warmed PBS and used as antigen to pulse the APCs for 2 hours at 37ºC in a 96-well V-shaped-bottom microplate at a concentration of $2x10^4$ cells per well. Antigen-pulsed APCs were pelleted, then incubated with T cell media with 100 µg/mL Gentamicin sulfate salt (Sigma, Catalog No. G1264) for 1 hour at 37ºC before washing and re-suspending in T cell media.

T cells: $CD4^+$ T cells were isolated from LN via EasySep™ Mouse $CD4^+$ T Cell Isolation Kit (Catalog No. 19852) and isolation efficiency was verified via flow cytometry. $CD4^+$ T cells were then labeled with the CellTrace™ Violet Cell Proliferation Kit (Invitrogen™, Catalog No. C34557) before co-culturing at 37ºC with antigen-pulsed, Gentamicin-washed APCs at a ratio of 10:1. After 48 hours of incubation, cells were harvested and stained for flow cytometry.

Photoconversion of Intestinal Cells

Photoconversion of intestinal tissue was performed in SPF *CAG::KikGr*[33] mice as previously described (Kitamoto et al., 2020; Nakanishi et al., 2018). Mice were anesthetized with isoflurane delivered in O_2 and body temperature was maintained at 37ºC via heating pad throughout the procedure. Abdominal area was shaved prior to making an incision in the abdominal wall to externalize the intestinal tissues (SI, colon, caecum, and gut-draining LN). The rest of the body was covered with aluminum foil to prevent non-specific labeling while only the intestinal tract was exposed to a violet laser

source (405 nm, peak power) for 1 minute. The intestinal tissues were returned back to the abdomen and the incision sutured. Mice were given post-operative pain medication. Twenty-four hours after surgery, cells from various tissues were analyzed via flow cytometry for presence of photoconverted RFP+ cells.

Adoptive Transfer of $CD4^+$ T cells

Donor $CD4^+$ T cells were isolated from gut-draining LN via EasySep™ Mouse $CD4^+$ T Cell Isolation Kit (Catalog No. 19852) and isolation efficiency was verified via flow cytometry. A total of $1x10^5$ $CD4^+$ T cells were injected intraperitoneally (i.p.) into recipient mice. Either twenty-four hours or 7 days after adoptive transfer, various tissues of recipient mice were harvested and stained cell suspensions were analyzed via flow cytometry for presence of donor $CD4^+$ T cells.

Tissue Processing and Flow Cytometry

Secondary lymphoid organs: Lymph nodes and spleen were harvested and then processed over sterile wire mesh in 2 mL of complete RPMI media before cell isolation and tetramer staining in PBS. Red blood cells in spleen were lysed with ACK lysing buffer prior to isolation.

Skin: Back skin was harvested, lightly defatted, then minced with scissors to a fine consistency before tissue digestion in 4 mL complete RPMI (RPMI plus 10% fetal calf serum, 1% penicillin-streptomycin, β-mercaptoethanol, glutamate, sodium pyruvate, HEPES and non-essential amino acids) then supplemented with 2 mg/mL collagenase XI, 0.5 mg/mL hyaluronidase, 0.1 mg/mL DNase. Digested skin samples were then

incubated, with shaking, at 37ºC for 45 minutes before quenching with 15 mL of complete RPMI media and shaking by hand for 30 seconds. Skin cell suspensions were filtered through sterile cell strainers (100 µM followed by 40 µM).

Colon LP: Lamina propria lymphocytes were isolated with minimal modifications to previous published work (Nayak et al., 2021). In brief, colons were harvested and fileted, then washed with 1 mL PBS to remove stool before resting in complete RPMI media. After rinsing with 1X HBSS (without Ca^{2+} and Mg^{2+}), colons were then each incubated, with shaking, in 15 mL 1X HBSS (without Ca^{2+} and Mg^{2+}) supplemented with 5 mM EDTA (Promega) and 1 mM DL-Dithiothreitol (DTT) (Bioplus chemicals) for 45 minutes at 37ºC in order to remove mucus. Samples were then filtered with a 100 µM sterile cell strainer to discard supernatant before tissue digestion for 45 minutes at 37°C in 15 mL each of 1X HBSS (with Ca^{2+} and Mg^{2+}) supplemented with 5% (v/v) fetal bovine serum (GIBCO heat inactivated), 1 U/mL Dispase (Sigma), 0.5 mg/mL Collagenase VIII (Sigma), and 20 µg/mL DNaseI (Sigma). After quenching with 15 mL of complete RPMI media, the supernatant was filtered over a 40 µM sterile cell strainer and collected in a new tube. Cell suspensions were pelleted 1,000 g for 10 minutes at 4ºC, then subjected to a Percoll (VWR) gradient (40%/80% [v/v]) before pelleting at 1,000 g for 20 minutes with no brake and no acceleration. Cells at the interface were collected and washed with PBS.

Cell counting: All tissues were re-suspended in 1 mL PBS and 25 µL of cell suspension was mixed with 25 µL of AccuCheck counting beads (Invitrogen, Catalog No. PCB100) for calculating absolute numbers of cells.

Antibody staining: Remaining cells were stained in PBS for 30 minutes at 4ºC with surface antibodies and a Live/Dead marker (Ghost Dye Violet 510, Tonbo Biosciences, Catalog No. 13-0870-T100). For intracellular staining, cells were fixed and permeabilized using the Foxp3 staining kit (eBioscience, Catalog No. 00-5523-00) buffer for 30 minutes at 4ºC then stained in permeabilization buffer for 30 minutes at 4ºC. Stained cells were run on a Fortessa (BD Biosciences) in the UCSF Flow Cytometry Core. Flow cytometry data was analyzed using FlowJo software (FlowJo, LLC).

Tetramer Staining and Enrichment

To identify 2W-specific cells, cell suspensions were pelleted and then stained for 1 hour at room temperature (15–25ºC), while protected from light, with a 2W1S:I-Ab–streptavidin-phycoerythrin (PE) tetramer at a concentration of 10 nM. Skin and colon LP were then directly stained for other surface and intracellular markers as described above. For LN samples, the tetramer-bound fraction was enriched via an adapted protocol of the EasySep PE Selection Kit II (StemCell Technologies, Inc.) developed by Marc Jenkins' lab. In brief, 6.25 µL of EasySep PE selection cocktail was added to each sample in a total volume of 500 mL and then incubated, while protected from light, at room temperature for 15 minutes. Cells were incubated for an additional 10 minutes after addition of 12.5 µL of EasySep magnetic particles. Finally, cell suspensions were brought up to a total volume of 2.5 mL with PBS and placed into the EasySep magnet for 5 minutes at room temperature. Supernatants (unbound fractions) were poured off into another collection tube. This process of washing with PBS and enriching for

magnetically-bound cells was repeated twice until the positively-selected cells (bound fraction) and pooled unbound fraction for each sample were taken for cell counting and staining.

Microbial sequencing and analysis

Sample processing: Mouse fecal samples (n=10) were submitted for DNA extraction, PCR amplification of the V4 hypervariable region of the 16S rRNA gene, and DNA sequencing on the Illumina MiSeq. DNA was extracted from all samples using a modified CTAB extraction protocol. Each DNA sample was amplified using primer pairs that (1) targeted the V4 hypervariable region of the 16S rRNA gene, (2) contained a unique barcode sequence to enable demultiplexing of pooled samples, and (3) contained an adapter sequence that enables the amplicon to bind to the MiSeq flow cell based on a previously published protocol [@shenoy_gut_2019]. Amplicons with sufficient DNA concentrations were pooled in equal molar concentrations and sequenced on the Illumina MiSeq.

Sequencing Data Processing: Aligned read pairs containing less than two expected errors were binned into OTUs (operational taxonomic units) using a 97% sequence similarity threshold. OTUs determined to be chimeric or of non-bacterial origin were discarded. Additionally, taxa known to be common contaminants (including, but not limited to, *Delftia* and *Pseudomonas*) and observed in greater than 50% of extraction controls were discarded. The maximum read count of each remaining OTU in any single extraction control was subtracted from the reads counts of that OTU for each sample. Read counts for OTUs which summed across all samples that were less than

0.001% of the total read count for the dataset were discarded to minimize noise in the dataset. Sample read numbers were representatively rarefied 100 times to 60,000 reads as a means of accounting for differences in sample read sizes, leaving 9 samples for analysis (One sample was negative control).

Bacterial enumeration

For CFU enumeration in Figure 3A, 100 mg of stool was directly obtained from harvested mouse colons and homogenized in 1 mL of sterile PBS via vortex. Bacterial suspensions were then plated on erythromycin-containing TSA to select for *S. epi*-2W mCherry and colonies were enumerated to quantify total CFUs.

Quantification and Statistical Analysis

The number of mice per group is annotated in each of the corresponding figure legends. Data followed a Gaussian distribution and variation was similar between groups for the conditions analyzed. Significance was assessed using the unpaired Student's t test or one-way ANOVA with a Tukey post-test in GraphPad Prism software (GraphPad). In all figures, the mean value is visually depicted. P values correlate with symbols as follows: ns = not significant, $p > 0.05$, * $p \leq 0.05$, ** $p \leq 0.01$, *** $p \leq 0.001$, **** $p \leq 0.0001$. Mice were allocated randomly into experimental groups after matching for age and gender.

CHAPTER 4: FUTURE DIRECTIONS

Cellular sources and targets of pro-inflammatory factors

In this work, we provide evidence for the importance of IL-1 signaling in skewing cutaneous antigen-specific responses during acute intestinal inflammation. Although intestinal-derived IL-1 is likely driving the majority of this response, there are potential cellular sources of this and other pro-inflammatory factors that are locally acting in the skin as well. Coincidentally, we found that mild skin injury was indispensable for our phenotype. One likely source of additional IL-1 in skin could be either keratinocytes or macrophages, which have both been shown to produce these molecules upon tape-stripping or skin injury (Archer et al., 2019; Wang et al., 2021).

Another avenue of investigation lies in the specific cellular targets of IL-1 signaling in the skin. Although we have shown the importance of the IL-1 receptor on $CD4^+$ T cells, we aim to further distinguish the role of Tregs and T effectors. IL-1 receptor signaling to Tregs leads to destabilization of this cell population (Alvarez et al., 2019), which begs the question of whether excess IL-1 could directly impact the function of *S. epi*-specific Tregs.

Changes in expression of gut and skin-homing receptors

We explored the role of T cell trafficking from gut to skin dLN in our model but have yet to comprehensively characterize changes in expression of gut and skin-homing receptors important in this movement (Fowell and Kim, 2021), such as α4β7 and CCR4 in mice. There exists a precedent for reprogramming of gut-homing receptors into skin-homing receptors (Oyoshi et al., 2011), though this has mainly been

studied in the context of allergy, making this avenue of investigation novel and intriguing. We can therefore characterize the pathways by which gut and skin-homing receptors could be reprogrammed in the context of host-microbe interactions.

Long-term consequences of altered response to *S. epidermidis*

Another aspect that warrants further investigation is the long-term consequence of the altered cutaneous response to *S. epidermidis*, especially as we have preliminary results suggesting that prior intestinal inflammation can have persisting effects on polyclonal $CD4^+$ T cell responses to *S. epidermidis*. Accumulation of commensal fungi-induced Th17 cells can increase susceptibility to psoriasis in mice (Hurabielle et al., 2020), so depending on the long-term stability of *S. epi*-specific effector CD4+ T cells, these cells could also contribute to pathogenesis in similar models of skin disease.

Skin to gut influence

Skin injury has been shown to promote anaphylaxis to oral antigens (Leyva-Castillo et al., 2019). An interesting aspect that warrants further investigation is the influence of skin inflammation on gut immune tolerance to commensal microbes. In conjunction with this project, we have engineered a gut commensal to express our model antigen 2W (*Bacteroides thetaiotaomicron*-2W), which makes this avenue of research plausible in the near future. We also have some preliminary data (not shown) in which we show that tape-stripping itself can worsen colitis pathogenesis, suggesting the influence of skin perturbation on overall intestinal inflammation.

Microbially-derived molecules with capacity to influence immune responses

Although there are clear differences in gut microbial community composition in our study, we have yet to profile these in the skin. In turn, these changes may reflect the altered immunomodulatory capacity of microbes present in the system, either locally in the gut and skin, or in circulation. We can therefore test the effects of intestinal *S. epidermidis* on other microbes, such as those which produce Treg-inducing metabolites in the gut, in the context of our DSS and skin re-challenge model. On the other hand, there also could be potential metabolic differences in intestinal versus skin *S. epidermidis* within the same host, as they inhabit and have to adapt to extremely different environments. In either case, performing metabolomics on gut and skin tissues would be informative in terms of which microbially-derived molecules could be potentially skewing the response to cutaneous *S. epidermidis* during gut inflammation.

REFERENCES

Adlerberth, I., Lindberg, E., Aberg, N., Hesselmar, B., Saalman, R., Strannegård, I. L., & Wold, A. E. (2006). Reduced enterobacterial and increased staphylococcal colonization of the infantile bowel: an effect of hygienic lifestyle?. *Pediatric research*, 59(1), 96–101.

Agace, W. W., & McCoy, K. D. (2017). Regionalized Development and Maintenance of the Intestinal Adaptive Immune Landscape. *Immunity*, 46(4), 532–548.

Akdis C. A. (2021). Does the epithelial barrier hypothesis explain the increase in allergy, autoimmunity and other chronic conditions?. *Nature reviews. Immunology*, 10.1038/s41577-021-00538-7. Advance online publication.

Al Nabhani, Z., Dulauroy, S., Marques, R., Cousu, C., Al Bounny, S., Déjardin, F., Sparwasser, T., Bérard, M., Cerf-Bensussan, N., & Eberl, G. (2019). A Weaning Reaction to Microbiota Is Required for Resistance to Immunopathologies in the Adult. *Immunity*, 50(5), 1276–1288.e5.

Alvarez, F., Istomine, R., Shourian, M., Pavey, N., Al-Aubodah, T. A., Qureshi, S., Fritz, J. H., & Piccirillo, C. A. (2019). The alarmins IL-1 and IL-33 differentially regulate the functional specialisation of Foxp3+ regulatory T cells during mucosal inflammation. *Mucosal immunology*, 12(3), 746–760.

Arai, Y., Takanashi, H., Kitagawa, H., & Okayasu, I. (1998). Involvement of interleukin-1 in the development of ulcerative colitis induced by dextran sulfate sodium in mice. *Cytokine*, 10(11), 890–896.

Archer, N. K., Jo, J. H., Lee, S. K., Kim, D., Smith, B., Ortines, R. V., Wang, Y., Marchitto, M. C., Ravipati, A., Cai, S. S., Dillen, C. A., Liu, H., Miller, R. J., Ashbaugh, A. G., Uppal, A. S., Oyoshi, M. K., Malhotra, N., Hoff, S., Garza, L. A.,

Kong, H. H., … Miller, L. S. (2019). Injury, dysbiosis, and filaggrin deficiency drive skin inflammation through keratinocyte IL-1α release. *The Journal of allergy and clinical immunology*, 143(4), 1426–1443.e6.

Atarashi, K., Tanoue, T., Ando, M., Kamada, N., Nagano, Y., Narushima, S., Suda, W., Imaoka, A., Setoyama, H., Nagamori, T., Ishikawa, E., Shima, T., Hara, T., Kado, S., Jinnohara, T., Ohno, H., Kondo, T., Toyooka, K., Watanabe, E., Yokoyama, S., … Honda, K. (2015). Th17 Cell Induction by Adhesion of Microbes to Intestinal Epithelial Cells. *Cell*, 163(2), 367–380.

Atarashi, K., Tanoue, T., Shima, T., Imaoka, A., Kuwahara, T., Momose, Y., Cheng, G., Yamasaki, S., Saito, T., Ohba, Y., Taniguchi, T., Takeda, K., Hori, S., Ivanov, I. I., Umesaki, Y., Itoh, K., & Honda, K. (2011). Induction of colonic regulatory T cells by indigenous Clostridium species. *Science* (New York, N.Y.), 331(6015), 337–341.

Ayres J. S. (2016). Cooperative Microbial Tolerance Behaviors in Host-Microbiota Mutualism. *Cell*, 165(6), 1323–1331.

Bacchetta, R., Passerini, L., Gambineri, E., Dai, M., Allan, S. E., Perroni, L., Dagna-Bricarelli, F., Sartirana, C., Matthes-Martin, S., Lawitschka, A., Azzari, C., Ziegler, S. F., Levings, M. K., & Roncarolo, M. G. (2006). Defective regulatory and effector T cell functions in patients with FOXP3 mutations. *The Journal of clinical investigation*, 116(6), 1713–1722.

Basu, R., Whitley, S. K., Bhaumik, S., Zindl, C. L., Schoeb, T. R., Benveniste, E. N., Pear, W. S., Hatton, R. D., & Weaver, C. T. (2015). IL-1 signaling modulates

activation of STAT transcription factors to antagonize retinoic acid signaling and control the TH17 cell-iTreg cell balance. *Nature immunology*, 16(3), 286–295.

Belkaid, Y., & Harrison, O. J. (2017). Homeostatic Immunity and the Microbiota. *Immunity*, 46(4), 562–576.

Ben-Sasson, S. Z., Hu-Li, J., Quiel, J., Cauchetaux, S., Ratner, M., Shapira, I., Dinarello, C. A., & Paul, W. E. (2009). IL-1 acts directly on CD4 T cells to enhance their antigen-driven expansion and differentiation. *Proceedings of the National Academy of Sciences of the United States of America*, 106(17), 7119–7124.

Bloom, S. M., Bijanki, V. N., Nava, G. M., Sun, L., Malvin, N. P., Donermeyer, D. L., Dunne, W. M., Jr, Allen, P. M., & Stappenbeck, T. S. (2011). Commensal Bacteroides species induce colitis in host-genotype-specific fashion in a mouse model of inflammatory bowel disease. *Cell host & microbe*, 9(5), 390–403.

Brown, H., & Esterházy, D. (2021). Intestinal immune compartmentalization: implications of tissue specific determinants in health and disease. *Mucosal immunology*, 10.1038/s41385-021-00420-8. Advance online publication.

Byrd, A. L., Belkaid, Y., & Segre, J. A. (2018). The human skin microbiome. *Nature reviews. Microbiology*, 16(3), 143–155.

Campbell, C., McKenney, P. T., Konstantinovsky, D., Isaeva, O. I., Schizas, M., Verter, J., Mai, C., Jin, W. B., Guo, C. J., Violante, S., Ramos, R. J., Cross, J. R., Kadaveru, K., Hambor, J., & Rudensky, A. Y. (2020). Bacterial metabolism of bile acids promotes generation of peripheral regulatory T cells. *Nature*, 581(7809), 475–479.

Cao, C., Yu, M., & Chai, Y. (2019). Pathological alteration and therapeutic implications of sepsis-induced immune cell apoptosis. *Cell death & disease*, 10(10), 782.

Chen, Y., Fischbach, M. & Belkaid, Y. (2018). Skin microbiota–host interactions. *Nature* 553**,** 427–436.

Chow, J., Tang, H., & Mazmanian, S. K. (2011). Pathobionts of the gastrointestinal microbiota and inflammatory disease. *Current opinion in immunology*, 23(4), 473–480.

Chung, Y., Chang, S. H., Martinez, G. J., Yang, X. O., Nurieva, R., Kang, H. S., Ma, L., Watowich, S. S., Jetten, A. M., Tian, Q., & Dong, C. (2009). Critical regulation of early Th17 cell differentiation by interleukin-1 signaling. *Immunity*, 30(4), 576–587.

Coates, M., Lee, M. J., Norton, D., & MacLeod, A. S. (2019). The Skin and Intestinal Microbiota and Their Specific Innate Immune Systems. *Frontiers in immunology*, 10, 2950.

De Pessemier, B., Grine, L., Debaere, M., Maes, A., Paetzold, B., & Callewaert, C. (2021). Gut-Skin Axis: Current Knowledge of the Interrelationship between Microbial Dysbiosis and Skin Conditions. *Microorganisms*, 9(2), 353.

Depner, M., Taft, D. H., Kirjavainen, P. V., Kalanetra, K. M., Karvonen, A. M., Peschel, S., Schmausser-Hechfellner, E., Roduit, C., Frei, R., Lauener, R., Divaret-Chauveau, A., Dalphin, J. C., Riedler, J., Roponen, M., Kabesch, M., Renz, H., Pekkanen, J., Farquharson, F. M., Louis, P., Mills, D. A., … Ege, M. J. (2020). Maturation of the gut microbiome during the first year of life contributes to the protective farm effect on childhood asthma. *Nature medicine*, 26(11), 1766–1775.

Dhariwala, M. O., Karthikeyan, D., Vasquez, K. S., Farhat, S., Weckel, A., Taravati, K., Leitner, E. G., Clancy, S., Pauli, M., Piper, M. L., Cohen, J. N., Ashouri, J. F., Lowe, M. M., Rosenblum, M. D., & Scharschmidt, T. C. (2020). Developing Human Skin Contains Lymphocytes Demonstrating a Memory Signature. *Cell reports. Medicine*, 1(8), 100132.

Di Domizio, J., Belkhodja, C., Chenuet, P., Fries, A., Murray, T., Mondéjar, P. M., Demaria, O., Conrad, C., Homey, B., Werner, S., Speiser, D. E., Ryffel, B., & Gilliet, M. (2020). The commensal skin microbiota triggers type I IFN-dependent innate repair responses in injured skin. *Nature immunology*, 21(9), 1034–1045.

Donaldson, G. P., Ladinsky, M. S., Yu, K. B., Sanders, J. G., Yoo, B. B., Chou, W. C., Conner, M. E., Earl, A. M., Knight, R., Bjorkman, P. J., & Mazmanian, S. K. (2018). Gut microbiota utilize immunoglobulin A for mucosal colonization. *Science* (New York, N.Y.), 360(6390), 795–800.

Durack, J., & Lynch, S. V. (2019). The gut microbiome: Relationships with disease and opportunities for therapy. *The Journal of experimental medicine*, 216(1), 20–40.

Dutzan, N., Abusleme, L., Bridgeman, H., Greenwell-Wild, T., Zangerle-Murray, T., Fife, M. E., Bouladoux, N., Linley, H., Brenchley, L., Wemyss, K., Calderon, G., Hong, B. Y., Break, T. J., Bowdish, D., Lionakis, M. S., Jones, S. A., Trinchieri, G., Diaz, P. I., Belkaid, Y., Konkel, J. E., … Moutsopoulos, N. M. (2017). On-going Mechanical Damage from Mastication Drives Homeostatic Th17 Cell Responses at the Oral Barrier. *Immunity*, 46(1), 133–147.

Eichele, D. D., & Kharbanda, K. K. (2017). Dextran sodium sulfate colitis murine model: An indispensable tool for advancing our understanding of inflammatory bowel diseases pathogenesis. *World journal of gastroenterology*, 23(33), 6016–6029.

Elinav, E., Strowig, T., Kau, A. L., Henao-Mejia, J., Thaiss, C. A., Booth, C. J., Peaper, D. R., Bertin, J., Eisenbarth, S. C., Gordon, J. I., & Flavell, R. A. (2011). NLRP6 inflammasome regulates colonic microbial ecology and risk for colitis. *Cell*, 145(5), 745–757.

Esterházy, D., Canesso, M., Mesin, L., Muller, P. A., de Castro, T., Lockhart, A., ElJalby, M., Faria, A., & Mucida, D. (2019). Compartmentalized gut lymph node drainage dictates adaptive immune responses. *Nature*, 569(7754), 126–130.

Faith, J. J., Guruge, J. L., Charbonneau, M., Subramanian, S., Seedorf, H., Goodman, A. L., Clemente, J. C., Knight, R., Heath, A. C., Leibel, R. L., Rosenbaum, M., & Gordon, J. I. (2013). The long-term stability of the human gut microbiota. *Science* (New York, N.Y.), 341(6141), 1237439.

Findley, K., Oh, J., Yang, J., Conlan, S., Deming, C., Meyer, J. A., Schoenfeld, D., Nomicos, E., Park, M., NIH Intramural Sequencing Center Comparative Sequencing Program, Kong, H. H., & Segre, J. A. (2013). Topographic diversity of fungal and bacterial communities in human skin. *Nature*, 498(7454), 367–370.

Flowers, L., & Grice, E. A. (2020). The Skin Microbiota: Balancing Risk and Reward. *Cell host & microbe*, 28(2), 190–200.

Fontenot, J. D., Gavin, M. A., & Rudensky, A. Y. (2003). Foxp3 programs the development and function of CD4+CD25+ regulatory T cells. *Nature immunology*, 4(4), 330–336.

Fowell, D. J., & Kim, M. (2021). The spatio-temporal control of effector T cell migration. *Nature reviews. Immunology*, 21(9), 582–596.

Fujimura, K. E., Sitarik, A. R., Havstad, S., Lin, D. L., Levan, S., Fadrosh, D., Panzer, A. R., LaMere, B., Rackaityte, E., Lukacs, N. W., Wegienka, G., Boushey, H. A., Ownby, D. R., Zoratti, E. M., Levin, A. M., Johnson, C. C., & Lynch, S. V. (2016). Neonatal gut microbiota associates with childhood multisensitized atopy and T cell differentiation. *Nature medicine*, 22(10), 1187–1191.

Gaffen, S. L., Jain, R., Garg, A. V., & Cua, D. J. (2014). The IL-23-IL-17 immune axis: from mechanisms to therapeutic testing. *Nature reviews. Immunology*, 14(9), 585–600.

Garcia-Gutierrez, E., Walsh, C. J., Sayavedra, L., Diaz-Calvo, T., Thapa, D., Ruas-Madiedo, P., Mayer, M. J., Cotter, P. D., & Narbad, A. (2020). Genotypic and Phenotypic Characterization of Fecal Staphylococcus epidermidis Isolates Suggests Plasticity to Adapt to Different Human Body Sites. *Frontiers in microbiology*, 11, 688.

Gimblet, C., Meisel, J. S., Loesche, M. A., Cole, S. D., Horwinski, J., Novais, F. O., Misic, A. M., Bradley, C. W., Beiting, D. P., Rankin, S. C., Carvalho, L. P., Carvalho, E. M., Scott, P., & Grice, E. A. (2017). Cutaneous Leishmaniasis Induces a Transmissible Dysbiotic Skin Microbiota that Promotes Skin Inflammation. *Cell host & microbe*, 22(1), 13–24.e4.

González-Navajas, J. M., Law, J., Nguyen, K. P., Bhargava, M., Corr, M. P., Varki, N., Eckmann, L., Hoffman, H. M., Lee, J., & Raz, E. (2010). Interleukin 1 receptor signaling regulates DUBA expression and facilitates Toll-like receptor 9-driven

antiinflammatory cytokine production. *The Journal of experimental medicine*, 207(13), 2799–2807.

Gopalakrishnan, V., Spencer, C. N., Nezi, L., Reuben, A., Andrews, M. C., Karpinets, T. V., Prieto, P. A., Vicente, D., Hoffman, K., Wei, S. C., Cogdill, A. P., Zhao, L., Hudgens, C. W., Hutchinson, D. S., Manzo, T., Petaccia de Macedo, M., Cotechini, T., Kumar, T., Chen, W. S., Reddy, S. M., … Wargo, J. A. (2018). Gut microbiome modulates response to anti-PD-1 immunotherapy in melanoma patients. *Science* (New York, N.Y.), 359(6371), 97–103.

Gregorio, J., Meller, S., Conrad, C., Di Nardo, A., Homey, B., Lauerma, A., Arai, N., Gallo, R. L., Digiovanni, J., & Gilliet, M. (2010). Plasmacytoid dendritic cells sense skin injury and promote wound healing through type I interferons. *The Journal of experimental medicine*, 207(13), 2921–2930.

Grice, E. A., Kong, H. H., Conlan, S., Deming, C. B., Davis, J., Young, A. C., NISC Comparative Sequencing Program, Bouffard, G. G., Blakesley, R. W., Murray, P. R., Green, E. D., Turner, M. L., & Segre, J. A. (2009). Topographical and temporal diversity of the human skin microbiome. *Science* (New York, N.Y.), 324(5931), 1190–1192.

Hand, T. W., Dos Santos, L. M., Bouladoux, N., Molloy, M. J., Pagán, A. J., Pepper, M., Maynard, C. L., Elson, C. O., 3rd, & Belkaid, Y. (2012). Acute gastrointestinal infection induces long-lived microbiota-specific T cell responses. *Science* (New York, N.Y.), 337(6101), 1553–1556.

Harrington, L. E., Hatton, R. D., Mangan, P. R., Turner, H., Murphy, T. L., Murphy, K. M., & Weaver, C. T. (2005). Interleukin 17-producing CD4+ effector T cells

develop via a lineage distinct from the T helper type 1 and 2 lineages. *Nature immunology*, 6(11), 1123–1132.

Harrison, O. J., Linehan, J. L., Shih, H. Y., Bouladoux, N., Han, S. J., Smelkinson, M., Sen, S. K., Byrd, A. L., Enamorado, M., Yao, C., Tamoutounour, S., Van Laethem, F., Hurabielle, C., Collins, N., Paun, A., Salcedo, R., O'Shea, J. J., & Belkaid, Y. (2019). Commensal-specific T cell plasticity promotes rapid tissue adaptation to injury. *Science* (New York, N.Y.), 363(6422).

Hild, B., Dreier, M.S., Oh, J.H. et al. Neonatal exposure to a wild-derived microbiome protects mice against diet-induced obesity. *Nat Metab* 3, 1042–1057 (2021).

Horai, R., Zárate-Bladés, C. R., Dillenburg-Pilla, P., Chen, J., Kielczewski, J. L., Silver, P. B., Jittayasothorn, Y., Chan, C.-C., Yamane, H., Honda, K., & Caspi, R. R. (2015). Microbiota-Dependent Activation of an Autoreactive T Cell Receptor Provokes Autoimmunity in an Immunologically Privileged Site. *Immunity*, 43(2), 343–353.

Hori, S., Nomura, T., & Sakaguchi, S. (2003). Control of regulatory T cell development by the transcription factor Foxp3. *Science* (New York, N.Y.), 299(5609), 1057–1061.

Houston, S. A., Cerovic, V., Thomson, C., Brewer, J., Mowat, A. M., & Milling, S. (2016). The lymph nodes draining the small intestine and colon are anatomically separate and immunologically distinct. *Mucosal immunology*, 9(2), 468–478.

Hoytema van Konijnenburg DP, Reis BS, Pedicord VA, Farache J, Victora GD, Mucida D. Intestinal Epithelial and Intraepithelial T Cell Crosstalk Mediates a Dynamic Response to Infection. *Cell*. 2017;171(4):783-794.e13.

Hurabielle, C., Link, V. M., Bouladoux, N., Han, S. J., Merrill, E. D., Lightfoot, Y. L., Seto, N., Bleck, C., Smelkinson, M., Harrison, O. J., Linehan, J. L., Tamoutounour, S., Lionakis, M. S., Kaplan, M. J., Nakajima, S., & Belkaid, Y. (2020). Immunity to commensal skin fungi promotes psoriasiform skin inflammation. *Proceedings of the National Academy of Sciences of the United States of America*, 117(28), 16465–16474.

Ivanov, I. I., Atarashi, K., Manel, N., Brodie, E. L., Shima, T., Karaoz, U., Wei, D., Goldfarb, K. C., Santee, C. A., Lynch, S. V., Tanoue, T., Imaoka, A., Itoh, K., Takeda, K., Umesaki, Y., Honda, K., & Littman, D. R. (2009). Induction of intestinal Th17 cells by segmented filamentous bacteria. *Cell*, 139(3), 485–498.

Ivanov, I. I., McKenzie, B. S., Zhou, L., Tadokoro, C. E., Lepelley, A., Lafaille, J. J., Cua, D. J., & Littman, D. R. (2006). The orphan nuclear receptor RORgammat directs the differentiation program of proinflammatory IL-17+ T helper cells. *Cell*, 126(6),

Jain, A., Song, R., Wakeland, E. K., & Pasare, C. (2018). T cell-intrinsic IL-1R signaling licenses effector cytokine production by memory CD4 T cells. *Nature communications*, 9(1), 3185.

Jiménez, E., Delgado, S., Maldonado, A., Arroyo, R., Albújar, M., García, N., Jariod, M., Fernández, L., Gómez, A., & Rodríguez, J. M. (2008). Staphylococcus epidermidis: a differential trait of the fecal microbiota of breast-fed infants. *BMC microbiology*, 8, 143.

Kalekar, L. A., Cohen, J. N., Prevel, N., Sandoval, P. M., Mathur, A. N., Moreau, J. M., Lowe, M. M., Nosbaum, A., Wolters, P. J., Haemel, A., Boin, F., & Rosenblum,

M. D. (2019). Regulatory T cells in skin are uniquely poised to suppress profibrotic immune responses. *Science immunology*, 4(39), eaaw2910.

Kattah, M. G., Shao, L., Rosli, Y. Y., Shimizu, H., Whang, M. I., Advincula, R., Achacoso, P., Shah, S., Duong, B. H., Onizawa, M., Tanbun, P., Malynn, B. A., & Ma, A. (2018). A20 and ABIN-1 synergistically preserve intestinal epithelial cell survival. *The Journal of experimental medicine*, 215(7), 1839–1852.

Khattri, R., Cox, T., Yasayko, S. A., & Ramsdell, F. (2003). An essential role for Scurfin in CD4+CD25+ T regulatory cells. *Nature immunology*, 4(4), 337–342.

Kiner, E., Willie, E., Vijaykumar, B., Chowdhary, K., Schmutz, H., Chandler, J., Schnell, A., Thakore, P. I., LeGros, G., Mostafavi, S., Mathis, D., Benoist, C., & Immunological Genome Project Consortium (2021). Gut CD4+ T cell phenotypes are a continuum molded by microbes, not by TH archetypes. *Nature immunology*, 22(2), 216–228.

Kitamoto, S., Nagao-Kitamoto, H., Jiao, Y., Gillilland, M. G., 3rd, Hayashi, A., Imai, J., Sugihara, K., Miyoshi, M., Brazil, J. C., Kuffa, P., Hill, B. D., Rizvi, S. M., Wen, F., Bishu, S., Inohara, N., Eaton, K. A., Nusrat, A., Lei, Y. L., Giannobile, W. V., & Kamada, N. (2020). The Intermucosal Connection between the Mouth and Gut in Commensal Pathobiont-Driven Colitis. *Cell*, 182(2), 447–462.e14.

Knoop, K. A., Gustafsson, J. K., McDonald, K. G., Kulkarni, D. H., Coughlin, P. E., McCrate, S., Kim, D., Hsieh, C. S., Hogan, S. P., Elson, C. O., Tarr, P. I., & Newberry, R. D. (2017). Microbial antigen encounter during a preweaning interval is critical for tolerance to gut bacteria. *Science immunology*, 2(18), eaao1314.

Kobayashi, T., Glatz, M., Horiuchi, K., Kawasaki, H., Akiyama, H., Kaplan, D. H., Kong, H. H., Amagai, M., & Nagao, K. (2015). Dysbiosis and Staphylococcus aureus Colonization Drives Inflammation in Atopic Dermatitis. *Immunity*, 42(4), 756–766.

Krebs, C. F., Paust, H.-J., Krohn, S., Koyro, T., Brix, S. R., Riedel, J.-H., Bartsch, P., Wiech, T., Meyer-Schwesinger, C., Huang, J., Fischer, N., Busch, P., Mittrücker, H.-W., Steinhoff, U., Stockinger, B., Perez, L. G., Wenzel, U. O., Janneck, M., Steinmetz, O. M., … Panzer, U. (2016). Autoimmune Renal Disease Is Exacerbated by S1P-Receptor-1-Dependent Intestinal Th17 Cell Migration to the Kidney. *Immunity*, 45(5), 1078–1092.

Kutlubay, Z., Tüzün, Y., & Wolf, R. (2017). The Pathergy Test as a Diagnostic Tool. *Skinmed*, 15(2), 97–104.

Lai, Y., Cogen, A. L., Radek, K. A., Park, H. J., Macleod, D. T., Leichtle, A., Ryan, A. F., Di Nardo, A., & Gallo, R. L. (2010). Activation of TLR2 by a small molecule produced by Staphylococcus epidermidis increases antimicrobial defense against bacterial skin infections. *The Journal of investigative dermatology*, 130(9), 2211–2221.

Langrish, C. L., Chen, Y., Blumenschein, W. M., Mattson, J., Basham, B., Sedgwick, J. D., McClanahan, T., Kastelein, R. A., & Cua, D. J. (2005). IL-23 drives a pathogenic T cell population that induces autoimmune inflammation. *The Journal of experimental medicine*, 201(2), 233–240.

Leech, J. M., Dhariwala, M. O., Lowe, M. M., Chu, K., Merana, G. R., Cornuot, C., Weckel, A., Ma, J. M., Leitner, E. G., Gonzalez, J. R., Vasquez, K. S., Diep, B. A., & Scharschmidt, T. C. (2019). Toxin-Triggered Interleukin-1 Receptor

Signaling Enables Early-Life Discrimination of Pathogenic versus Commensal Skin Bacteria. *Cell host & microbe*, 26(6), 795–809.e5.

Lehner, M. D., Ittner, J., Bundschuh, D. S., van Rooijen, N., Wendel, A., & Hartung, T. (2001). Improved innate immunity of endotoxin-tolerant mice increases resistance to Salmonella enterica serovar typhimurium infection despite attenuated cytokine response. *Infection and immunity*, 69(1), 463–471.

Leyva-Castillo, J. M., Galand, C., Kam, C., Burton, O., Gurish, M., Musser, M. A., Goldsmith, J. D., Hait, E., Nurko, S., Brombacher, F., Dong, C., Finkelman, F. D., Lee, R. T., Ziegler, S., Chiu, I., Austen, K. F., & Geha, R. S. (2019). Mechanical Skin Injury Promotes Food Anaphylaxis by Driving Intestinal Mast Cell Expansion. *Immunity*, 50(5), 1262–1275.e4.

Ligumsky, M., Simon, P. L., Karmeli, F., & Rachmilewitz, D. (1990). Role of interleukin 1 in inflammatory bowel disease--enhanced production during active disease. *Gut*, 31(6), 686–689.

Lukens, J. R., Vogel, P., Johnson, G. R., Kelliher, M. A., Iwakura, Y., Lamkanfi, M., & Kanneganti, T. D. (2013). RIP1-driven autoinflammation targets IL-1α independently of inflammasomes and RIP3. *Nature*, 498(7453), 224–227.

Macpherson, A. J., & Harris, N. L. (2004). Interactions between commensal intestinal bacteria and the immune system. *Nature reviews. Immunology*, 4(6), 478–485.

Malhotra, N., Leyva-Castillo, J. M., Jadhav, U., Barreiro, O., Kam, C., O'Neill, N. K., Meylan, F., Chambon, P., von Andrian, U. H., Siegel, R. M., Wang, E. C., Shivdasani, R., & Geha, R. S. (2018). RORα-expressing T regulatory cells restrain allergic skin inflammation. *Science immunology*, 3(21), eaao6923.

Man S. M. (2018). Inflammasomes in the gastrointestinal tract: infection, cancer and gut microbiota homeostasis. *Nature reviews. Gastroenterology & hepatology*, 15(12), 721–737.

Marzano, A. V., Borghi, A., Stadnicki, A., Crosti, C., & Cugno, M. (2014). Cutaneous manifestations in patients with inflammatory bowel diseases: pathophysiology, clinical features, and therapy. *Inflammatory bowel diseases*, 20(1), 213–227.

Marzano, A. V., Ortega-Loayza, A. G., Heath, M., Morse, D., Genovese, G., & Cugno, M. (2019). Mechanisms of Inflammation in Neutrophil-Mediated Skin Diseases. *Frontiers in immunology*, 10, 1059.

Mathur, A. N., Zirak, B., Boothby, I. C., Tan, M., Cohen, J. N., Mauro, T. M., Mehta, P., Lowe, M. M., Abbas, A. K., Ali, N., & Rosenblum, M. D. (2019). Treg-Cell Control of a CXCL5-IL-17 Inflammatory Axis Promotes Hair-Follicle-Stem-Cell Differentiation During Skin-Barrier Repair. *Immunity*, 50(3), 655–667.e4.

Matloubian, M., Lo, C. G., Cinamon, G., Lesneski, M. J., Xu, Y., Brinkmann, V., Allende, M. L., Proia, R. L., & Cyster, J. G. (2004). Lymphocyte egress from thymus and peripheral lymphoid organs is dependent on S1P receptor 1. *Nature*, 427(6972), 355–360.

Mazmanian, S. K., Liu, C. H., Tzianabos, A. O., & Kasper, D. L. (2005). An immunomodulatory molecule of symbiotic bacteria directs maturation of the host immune system. *Cell*, 122(1), 107–118.

McEntee, C. P., Finlay, C. M., & Lavelle, E. C. (2019). Divergent Roles for the IL-1 Family in Gastrointestinal Homeostasis and Inflammation. *Frontiers in immunology*, 10, 1266.

Menghini, P., Corridoni, D., Buttó, L. F., Osme, A., Shivaswamy, S., Lam, M., Bamias, G., Pizarro, T. T., Rodriguez-Palacios, A., Dinarello, C. A., & Cominelli, F. (2019). Neutralization of IL-1α ameliorates Crohn's disease-like ileitis by functional alterations of the gut microbiome. *Proceedings of the National Academy of Sciences of the United States of America*, 116(52), 26717–26726.

Merad, M., Ginhoux, F., & Collin, M. (2008). Origin, homeostasis and function of Langerhans cells and other langerin-expressing dendritic cells. *Nature reviews. Immunology*, 8(12), 935–947.

Mishra, A., Lai, G. C., Yao, L. J., Aung, T. T., Shental, N., Rotter-Maskowitz, A., Shepherdson, E., Singh, G., Pai, R., Shanti, A., Wong, R., Lee, A., Khyriem, C., Dutertre, C. A., Chakarov, S., Srinivasan, K. G., Shadan, N. B., Zhang, X. M., Khalilnezhad, S., Cottier, F., … Ginhoux, F. (2021). Microbial exposure during early human development primes fetal immune cells. *Cell*, 184(13), 3394–3409.e20.

Morton, A. M., Sefik, E., Upadhyay, R., Weissleder, R., Benoist, C., & Mathis, D. (2014). Endoscopic photoconversion reveals unexpectedly broad leukocyte trafficking to and from the gut. *Proceedings of the National Academy of Sciences*, 111(18), 6696–6701.

Muñoz-Rojas, A. R., & Mathis, D. (2021). Tissue regulatory T cells: regulatory chameleons. *Nature reviews. Immunology*, 10.1038/s41577-021-00519-w. Advance online publication.

Myers, B., Brownstone, N., Reddy, V., Chan, S., Thibodeaux, Q., Truong, A., Bhutani, T., Chang, H. W., & Liao, W. (2019). The gut microbiome in psoriasis and psoriatic arthritis. *Best practice & research. Clinical rheumatology*, 33(6), 101494.

Naik, S., Bouladoux, N., Linehan, J. L., Han, S. J., Harrison, O. J., Wilhelm, C., Conlan, S., Himmelfarb, S., Byrd, A. L., Deming, C., Quinones, M., Brenchley, J. M., Kong, H. H., Tussiwand, R., Murphy, K. M., Merad, M., Segre, J. A., & Belkaid, Y. (2015). Commensal-dendritic-cell interaction specifies a unique protective skin immune signature. *Nature*, 520(7545), 104–108.

Naik, S., Bouladoux, N., Wilhelm, C., Molloy, M. J., Salcedo, R., Kastenmuller, W., Deming, C., Quinones, M., Koo, L., Conlan, S., Spencer, S., Hall, J. A., Dzutsev, A., Kong, H., Campbell, D. J., Trinchieri, G., Segre, J. A., & Belkaid, Y. (2012). Compartmentalized Control of Skin Immunity by Resident Commensals. *Science* (New York, N.Y.), 337(6098), 1115–1119.

Nakanishi, Y., Ikebuchi, R., Chtanova, T., Kusumoto, Y., Okuyama, H., Moriya, T., Honda, T., Kabashima, K., Watanabe, T., Sakai, Y., & Tomura, M. (2018). Regulatory T cells with superior immunosuppressive capacity emigrate from the inflamed colon to draining lymph nodes. *Mucosal immunology*, 11(2), 437–448.

Napier, B. A., Andres-Terre, M., Massis, L. M., Hryckowian, A. J., Higginbottom, S. K., Cumnock, K., Casey, K. M., Haileselassie, B., Lugo, K. A., Schneider, D. S., Sonnenburg, J. L., & Monack, D. M. (2019). Western diet regulates immune status and the response to LPS-driven sepsis independent of diet-associated microbiome. *Proceedings of the National Academy of Sciences of the United States of America*, 116(9), 3688–3694.

Nayak, R. R., Alexander, M., Deshpande, I., Stapleton-Gray, K., Rimal, B., Patterson, A. D., Ubeda, C., Scher, J. U., & Turnbaugh, P. J. (2021). Methotrexate impacts conserved pathways in diverse human gut bacteria leading to decreased host immune activation. *Cell host & microbe*, 29(3), 362–377.e11.

Niess, J. H., Brand, S., Gu, X., Landsman, L., Jung, S., McCormick, B. A., Vyas, J. M., Boes, M., Ploegh, H. L., Fox, J. G., Littman, D. R., & Reinecker, H. C. (2005). CX3CR1-mediated dendritic cell access to the intestinal lumen and bacterial clearance. *Science* (New York, N.Y.), 307(5707), 254–258.

Nowotschin, S., & Hadjantonakis, A. K. (2009). Use of KikGR a photoconvertible green-to-red fluorescent protein for cell labeling and lineage analysis in ES cells and mouse embryos. *BMC developmental biology*, 9, 49.

O'Neill, C. A., Monteleone, G., McLaughlin, J. T., & Paus, R. (2016). The gut-skin axis in health and disease: A paradigm with therapeutic implications. *BioEssays : news and reviews in molecular, cellular and developmental biology*, 38(11), 1167–1176.

Oh, J., Byrd, A. L., Park, M., NISC Comparative Sequencing Program, Kong, H. H., & Segre, J. A. (2016). Temporal Stability of the Human Skin Microbiome. *Cell*, 165(4), 854–866.

Oyoshi, M. K., Elkhal, A., Scott, J. E., Wurbel, M. A., Hornick, J. L., Campbell, J. J., & Geha, R. S. (2011). Epicutaneous challenge of orally immunized mice redirects antigen-specific gut-homing T cells to the skin. *The Journal of clinical investigation*, 121(6), 2210–2220.

Park, H., Li, Z., Yang, X. O., Chang, S. H., Nurieva, R., Wang, Y. H., Wang, Y., Hood, L., Zhu, Z., Tian, Q., & Dong, C. (2005). A distinct lineage of CD4 T cells regulates tissue inflammation by producing interleukin 17. *Nature immunology*, 6(11), 1133–1141.

Powrie, F., Leach, M. W., Mauze, S., Caddle, L. B., & Coffman, R. L. (1993). Phenotypically distinct subsets of CD4+ T cells induce or protect from chronic intestinal inflammation in C. B-17 scid mice. *International immunology*, 5(11), 1461–1471.

Rackaityte, E., Halkias, J., Fukui, E. M., Mendoza, V. F., Hayzelden, C., Crawford, E. D., Fujimura, K. E., Burt, T. D., & Lynch, S. V. (2020). Viable bacterial colonization is highly limited in the human intestine in utero. *Nature medicine*, 26(4), 599–607.

Raffin, C., Vo, L. T., & Bluestone, J. A. (2020). T_{reg} cell-based therapies: challenges and perspectives. *Nature reviews. Immunology*, 20(3), 158–172.

Ridaura, V. K., Bouladoux, N., Claesen, J., Chen, Y. E., Byrd, A. L., Constantinides, M. G., Merrill, E. D., Tamoutounour, S., Fischbach, M. A., & Belkaid, Y. (2018). Contextual control of skin immunity and inflammation by Corynebacterium. *The Journal of experimental medicine*, 215(3), 785–799.

Rigoni, R., Fontana, E., Dobbs, K., Marrella, V., Taverniti, V., Maina, V., Facoetti, A., D'Amico, G., Al-Herz, W., Cruz-Munoz, M. E., Schuetz, C., Gennery, A. R., Garabedian, E. K., Giliani, S., Draper, D., Dbaibo, G., Geha, R. S., Meyts, I., Tousseyn, T., Neven, B., … Cassani, B. (2020). Cutaneous barrier leakage and

gut inflammation drive skin disease in Omenn syndrome. *The Journal of allergy and clinical immunology*, 146(5), 1165–1179.e11.

Rosenblum, M. D., Way, S. S., & Abbas, A. K. (2016). Regulatory T cell memory. *Nature reviews. Immunology*, 16(2), 90–101.

Round, J. L., & Mazmanian, S. K. (2010). Inducible Foxp3+ regulatory T-cell development by a commensal bacterium of the intestinal microbiota. *Proceedings of the National Academy of Sciences of the United States of America*, 107(27), 12204–12209.

Russell, S. L., Gold, M. J., Hartmann, M., Willing, B. P., Thorson, L., Wlodarska, M., Gill, N., Blanchet, M. R., Mohn, W. W., McNagny, K. M., & Finlay, B. B. (2012). Early life antibiotic-driven changes in microbiota enhance susceptibility to allergic asthma. *EMBO reports*, 13(5), 440–447.

Sá, D. C., & Festa, C., Neto (2016). Inflammasomes and dermatology. *Anais brasileiros de dermatologia*, 91(5), 566–578.

Salem, I., Ramser, A., Isham, N., & Ghannoum, M. A. (2018). The Gut Microbiome as a Major Regulator of the Gut-Skin Axis. *Frontiers in microbiology*, 9, 1459.

Scharschmidt, T. C., Vasquez, K. S., Pauli, M. L., Leitner, E. G., Chu, K., Truong, H. A., Lowe, M. M., Sanchez Rodriguez, R., Ali, N., Laszik, Z. G., Sonnenburg, J. L., Millar, S. E., & Rosenblum, M. D. (2017). Commensal Microbes and Hair Follicle Morphogenesis Coordinately Drive Treg Migration into Neonatal Skin. *Cell host & microbe*, 21(4), 467–477.e5.

Scharschmidt, T. C., Vasquez, K. S., Truong, H. A., Gearty, S. V., Pauli, M. L., Nosbaum, A., Gratz, I. K., Otto, M., Moon, J. J., Liese, J., Abbas, A. K.,

Fischbach, M. A., & Rosenblum, M. D. (2015). A Wave of Regulatory T Cells into Neonatal Skin Mediates Tolerance to Commensal Microbes. *Immunity*, 43(5), 1011–1021.

Schwarz, A., Bruhs, A., & Schwarz, T. (2017). The Short-Chain Fatty Acid Sodium Butyrate Functions as a Regulator of the Skin Immune System. *The Journal of investigative dermatology*, 137(4), 855–864.

Seo, S. U., Kamada, N., Muñoz-Planillo, R., Kim, Y. G., Kim, D., Koizumi, Y., Hasegawa, M., Himpsl, S. D., Browne, H. P., Lawley, T. D., Mobley, H. L., Inohara, N., & Núñez, G. (2015). Distinct Commensals Induce Interleukin-1β via NLRP3 Inflammasome in Inflammatory Monocytes to Promote Intestinal Inflammation in Response to Injury. *Immunity*, 42(4), 744–755.

Smith, P. M., Howitt, M. R., Panikov, N., Michaud, M., Gallini, C. A., Bohlooly-Y, M., Glickman, J. N., & Garrett, W. S. (2013). The microbial metabolites, short-chain fatty acids, regulate colonic Treg cell homeostasis. *Science* (New York, N.Y.), 341(6145), 569–573.

Song, H., Yoo, Y., Hwang, J., Na, Y. C., & Kim, H. S. (2016). Faecalibacterium prausnitzii subspecies-level dysbiosis in the human gut microbiome underlying atopic dermatitis. *The Journal of allergy and clinical immunology*, 137(3), 852–860.

Stockinger, B., & Omenetti, S. (2017). The dichotomous nature of T helper 17 cells. *Nature reviews. Immunology*, 17(9), 535–544.

Su, L. F., Del Alcazar, D., Stelekati, E., Wherry, E. J., & Davis, M. M. (2016). Antigen exposure shapes the ratio between antigen-specific Tregs and conventional T

cells in human peripheral blood. *Proceedings of the National Academy of Sciences of the United States of America*, 113(41), E6192–E6198.

Tanaka, A., & Sakaguchi, S. (2019). Targeting Treg cells in cancer immunotherapy. *European journal of immunology*, 49(8), 1140–1146.

Tropini, C., Earle, K. A., Huang, K. C., & Sonnenburg, J. L. (2017). The Gut Microbiome: Connecting Spatial Organization to Function. *Cell host & microbe*, 21(4), 433–442.

Tuganbaev, T., & Honda, K. (2021). Non-zero-sum microbiome immune system interactions. *European journal of immunology*, 10.1002/eji.202049065. Advance online publication.

Wang, G., Sweren, E., Liu, H., Wier, E., Alphonse, M. P., Chen, R., Islam, N., Li, A., Xue, Y., Chen, J., Park, S., Chen, Y., Lee, S., Wang, Y., Wang, S., Archer, N. K., Andrews, W., Kane, M. A., Dare, E., Reddy, S. K., … Garza, L. A. (2021). Bacteria induce skin regeneration via IL-1β signaling. *Cell host & microbe*, 29(5), 777–791.e6. https://doi.org/10.1016/j.chom.2021.03.003

Wilmore, J. R., Gaudette, B. T., Gomez Atria, D., Hashemi, T., Jones, D. D., Gardner, C. A., Cole, S. D., Misic, A. M., Beiting, D. P., & Allman, D. (2018). Commensal Microbes Induce Serum IgA Responses that Protect against Polymicrobial Sepsis. *Cell host & microbe*, 23(3), 302–311.e3.

Wing, J. B., Tanaka, A., & Sakaguchi, S. (2019). Human FOXP3^{+} Regulatory T Cell Heterogeneity and Function in Autoimmunity and Cancer. *Immunity*, 50(2), 302–316.

Wirtz, S., Popp, V., Kindermann, M. et al. Chemically induced mouse models of acute and chronic intestinal inflammation. *Nat Protoc* 12, 1295–1309 (2017).

Wu, H. J., Ivanov, I. I., Darce, J., Hattori, K., Shima, T., Umesaki, Y., Littman, D. R., Benoist, C., & Mathis, D. (2010). Gut-residing segmented filamentous bacteria drive autoimmune arthritis via T helper 17 cells. *Immunity*, 32(6), 815–827.

Xu, M., Pokrovskii, M., Ding, Y., Yi, R., Au, C., Harrison, O. J., Galan, C., Belkaid, Y., Bonneau, R., & Littman, D. R. (2018). c-MAF-dependent regulatory T cells mediate immunological tolerance to a gut pathobiont. *Nature*, 554(7692), 373–377.

Zegarra-Ruiz, D. F., Kim, D. V., Norwood, K., Kim, M., Wu, W. H., Saldana-Morales, F. B., Hill, A. A., Majumdar, S., Orozco, S., Bell, R., Round, J. L., Longman, R. S., Egawa, T., Bettini, M. L., & Diehl, G. E. (2021). Thymic development of gut-microbiota-specific T cells. *Nature*, 594(7863), 413–417.

Publishing Agreement

It is the policy of the University to encourage open access and broad distribution of all theses, dissertations, and manuscripts. The Graduate Division will facilitate the distribution of UCSF theses, dissertations, and manuscripts to the UCSF Library for open access and distribution. UCSF will make such theses, dissertations, and manuscripts accessible to the public and will take reasonable steps to preserve these works in perpetuity.

I hereby grant the non-exclusive, perpetual right to The Regents of the University of California to reproduce, publicly display, distribute, preserve, and publish copies of my thesis, dissertation, or manuscript in any form or media, now existing or later derived, including access online for teaching, research, and public service purposes.

DocuSigned by:

EAD2198225E8465...

Author Signature

9/1/2021

Date